REMARKS/ARGUMENTS

Claim 1 has been amended. Claims 4-37 have been canceled without prejudice. Claims 1-3 are now pending. No new matter has been inserted. Support for the amendment to claim 1 can be found at least at page 3, line 19 and page 6, line 4.

Reconsideration of the pending claims is respectfully requested in view of the above amendment and the following comments.

35 U.S.C. § 112, first paragraph

The Examiner rejected claims 1-3 under 35 U.S.C. § 112, first paragraph, based on the written description requirement. Applicant respectfully traverses this rejection.

While not conceding the correctness of the Examiner's position, in the interest of advancing prosecution, Applicant has amended claim 1 to recite a native Q2 and a native β-amyloid. To the extent that this rejection applies to the amended claims, the following comments are provided.

The Examiner states "not a single amino acid sequence of any Q2 or β-amyloid protein, nor gene sequence encoding such, is provided in the instant specification." In reply, Applicant points out that a "patent need not teach, and preferably omits, what is well-known in the art." Hybritech, Inc. v. Monoclonal Antibodies, Inc., 802 F.2d 1367, 1384, 231 USPQ 81, 94 (Fed. Cir. 1986), cert. denied, 480 U.S. 947 (1987). Moreover, "the written description requirement does not require the applicant to describe exactly the subject matter claimed, [instead] the description must clearly allow persons of ordinary skill in the art to recognize that [he or she] invented what is claimed." Union Oil Co. of Cal. v. Atlantic Richfield Co., 208 F.3d 989, 997, 54 USPQ2d 1227, 1232 (Fed. Cir. 2000) (emphasis added). Therefore, because the amino acid sequences of native Q2 and native β-amyloid protein are well known to those of skill in the art, there is no need to include them in the specification and the written description rejection should be withdrawn.

As disclosed in the specification at page 6, lines 2-5, ERp57/GRP58 is also known as TPDO-Q2, or just Q2. To illustrate the point that it is well known, a brief search of the protein database at the NCBI website (www.ncbi.nih.gov) reveals multiple references regarding ERp57 and its sequence. A copy of the results from the NCBI website is provided for the convenience

of the Examiner (Exhibit A). As a further example, see Hirano et al., Molecular cloning of the human glucose-regulated protein ERp57/GRP58, a thiol-dependent reductase, Eur. J. Biochem. 234 (1), 336-342 (1995) (Exhibit B). Hirano et al. discloses the sequences for ERp57/GRP58 in humans, cows, rats, and mice. See Hirano et al., at p. 339, Fig. 2.

The sequences for amyloid precursor protein, β-amyloid, β-amyloid 1-42, and β-amyloid 1-38 were also well known in the art before the filing date of the present application. For example, the table at col. 1 of USPN 5,750,349 (Suzuki et al.) (Exhibit C) discloses sequences for various β-amyloids as SEQ ID NO's 1-6 at col. 1. Many other references also establish that such sequences were well known. See, for example, the sequences of other native variants of β-amyloid such as the sequence of β-amyloid 1-40 in Malinchik et al., Biophysical J., 74:537-545 (1998) at p. 543, Fig. 7 (Exhibit D). See also, USPN 5,707,821 (Exhibit E), wherein the sequences of β-amyloid 1-40 and 1-42 are disclosed as SEQ ID NO's 2 and 1, respectively, and USPN 5,223,482, col. 2 (Exhibit F), where knowledge of the sequences is discussed.

Accordingly, Applicant submits that the sequences of Q2 and β-amyloid were well known by those of skill in the art before the filing date of the present application. Therefore, these sequences need not be stated in the specification and the written description for the pending claims has been satisfied. Applicant respectfully requests that this rejection be withdrawn.

Claims 1-3 were rejected under 35 U.S.C. § 112, first paragraph, as not enabled. Applicant respectfully traverses this rejection.

While conceding that the specification is enabling for claims drawn to structurally definable chaperon Q2 and β-amyloid polypeptide complexes, the Examiner alleges that the specification does not provide enablement for any complex comprising biologically functional equivalent forms of Q2 or β-amyloid with no known or recited structural and functional characteristics.

While not conceding the correctness of the Examiner's position, in the interest of advancing prosecution, Applicants have amended claim 1 to recite a native Q2 and a native β-amyloid. Accordingly, randomly mutated non-native Q2 or β-amyloid related polypeptides should no longer be of concern to the Examiner. As such, Applicants assert that the claims are sufficiently enabled. To the extent that this rejection still applies, the following comments are provided.

The Examiner states that the terms β-amyloid and Q2, alone, do not sufficiently characterize and enable the full scope of the polypeptides encompassed by the current claim language because of the inclusion of the terms "in a variety of forms" and "variant forms" in describing their meaning.

First, the claims are drawn to an isolated complex and Applicant has provided a working example at Example 3, page 17. Second, the claims now include the feature "native" and Exhibits A-F above show that such native β-amyloid and Q2 were well known in the art. As native β-amyloid was well known in the art, the scope of the claims is sufficiently enabled.

For a further example of native β-amyloid, see Haass et al., J. Bio. Chem., 268(5):3021-3024 (1993) (Exhibit G), who disclose that β-amyloid is derived from β-amyloid precursor protein and show multiple native β-amyloids. See Haass et al., at 3021. Because many variant forms were indeed known by those of skill in the art, a statement to this effect in the specification does not render the present claims non-enabled.

Finally, in objecting that the present claims as drafted encompass randomly mutated Q2 or β-amyloid related polypeptides that possess none of the desired functions of the instant invention, the Examiner cites the 1976 Rudinger reference for the proposition that the significance of particular amino acid sequences for different aspects of biological activity cannot be predicted a priori but must be determined from case to case by painstaking experimental study. In reply, Applicants assert that the skill in the art has advanced significantly in the over twenty years from the date of the reference to the filing date of the present application.

In light of the foregoing Amendment and Remarks, Applicants' assert the claims are in condition for allowance. Removal of all rejections and early notice of allowable claims is requested.

The Examiner is invited to telephone the undersigned attorney for clarification of any of these remarks or amendments, or to otherwise speed prosecution of this case.

Respectfully submitted,

MERCHANT & GOULD P.C.
P.O. Box 2903
Minneapolis, MN 55402-0903
(612) 332-5300

Date: Oct 23, 2003

Mark T. Skoog
Reg. No. 40,178
MTS:MED:kf

CUSTOMER NUMBER 23552

Attached: Exhibits A-G -

☐ 1: NP_005304. glucose regulated...[gi:21361657] BLink, Domains, Lin

```
LOCUS       NP_005304                505 aa            linear   PRI 05-OCT-2003
DEFINITION  glucose regulated protein, 58kDa [Homo sapiens].
ACCESSION   NP_005304
VERSION     NP_005304.3  GI:21361657
DBSOURCE    REFSEQ: accession NM_005313.3
KEYWORDS    .
SOURCE      Homo sapiens (human)
  ORGANISM  Homo sapiens
            Eukaryota; Metazoa; Chordata; Craniata; Vertebrata; Euteleostomi;
            Mammalia; Eutheria; Primates; Catarrhini; Hominidae; Homo.
REFERENCE   1  (residues 1 to 505)
  AUTHORS   Radcliffe,C.M., Diedrich,G., Harvey,D.J., Dwek,R.A., Cresswell,P.
            and Rudd,P.M.
  TITLE     Identification of specific glycoforms of major histocompatibility
            complex class I heavy chains suggests that class I peptide loading
            is an adaptation of the quality control pathway involving
            calreticulin and ERp57
  JOURNAL   J. Biol. Chem. 277 (48), 46415-46423 (2002)
  MEDLINE   22336355
   PUBMED   12235131
  REMARK    GeneRIF: role in class I loading process
REFERENCE   2  (residues 1 to 505)
  AUTHORS   Kang,S.J. and Cresswell,P.
  TITLE     Calnexin, calreticulin, and ERp57 cooperate in disulfide bond
            formation in human CD1d heavy chain
  JOURNAL   J. Biol. Chem. 277 (47), 44838-44844 (2002)
  MEDLINE   22323285
   PUBMED   12239218
  REMARK    GeneRIF: Data show that CD1d associates in the ER with both
            calnexin and calreticulin and with the thiol oxidoreductase ERp57
            in a manner dependent on glucose trimming of its N-linked glycans.
REFERENCE   3  (residues 1 to 505)
  AUTHORS   Okudo,H., Kito,M., Moriyama,T., Ogawa,T. and Urade,R.
  TITLE     Transglutaminase activity of human ER-60
  JOURNAL   Biosci. Biotechnol. Biochem. 66 (6), 1423-1426 (2002)
  MEDLINE   22152208
   PUBMED   12162574
  REMARK    GeneRIF: Transglutaminase activity of human ER-60
REFERENCE   4  (residues 1 to 505)
  AUTHORS   Antoniou,A.N., Ford,S., Alphey,M., Osborne,A., Elliott,T. and
            Powis,S.J.
  TITLE     The oxidoreductase ERp57 efficiently reduces partially folded in
            preference to fully folded MHC class I molecules
  JOURNAL   EMBO J. 21 (11), 2655-2663 (2002)
  MEDLINE   22027700
   PUBMED   12032078
  REMARK    GeneRIF: The oxidoreductase ERp57 efficiently reduces partially
            folded in preference to fully folded MHC class I molecules.
REFERENCE   5  (residues 1 to 505)
  AUTHORS   Guo,G.G., Patel,K., Kumar,V., Shah,M., Fried,V.A., Etlinger,J.D.
            and Sehgal,P.B.
```

TITLE Association of the chaperone glucose-regulated protein 58 (GRP58/ER-60/ERp57) with Stat3 in cytosol and plasma membrane complexes
JOURNAL J. Interferon Cytokine Res. 22 (5), 555-563 (2002)
MEDLINE 22055364
PUBMED 12060494
REMARK GeneRIF: Stat3 and GRP58 were observed to be coassociated with cytoplasmic membranes

REFERENCE 6 (residues 1 to 505)
AUTHORS Frickel,E.M., Riek,R., Jelesarov,I., Helenius,A., Wuthrich,K. and Ellgaard,L.
TITLE TROSY-NMR reveals interaction between ERp57 and the tip of the calreticulin P-domain
JOURNAL Proc. Natl. Acad. Sci. U.S.A. 99 (4), 1954-1959 (2002)
MEDLINE 21843878
PUBMED 11842220
REMARK GeneRIF: We found that ERp57 binds to the P-domain of calreticulin, an independently folding domain comprising residues 189-288.

REFERENCE 7 (residues 1 to 505)
AUTHORS Urade,R., Oda,T., Ito,H., Moriyama,T., Utsumi,S. and Kito,M.
TITLE Functions of characteristic Cys-Gly-His-Cys (CGHC) and Gln-Glu-Asp-Leu (QEDL) motifs of microsomal ER-60 protease
JOURNAL J. Biochem. 122 (4), 834-842 (1997)
MEDLINE 98060510
PUBMED 9399589

REFERENCE 8 (residues 1 to 505)
AUTHORS Koivunen,P., Horelli-Kuitunen,N., Helaakoski,T., Karvonen,P., Jaakkola,M., Palotie,A. and Kivirikko,K.I.
TITLE Structures of the human gene for the protein disulfide isomerase-related polypeptide ERp60 and a processed gene and assignment of these genes to 15q15 and 1q21
JOURNAL Genomics 42 (3), 397-404 (1997)
MEDLINE 97349107
PUBMED 9205111

REFERENCE 9 (residues 1 to 505)
AUTHORS Oliver,J.D., van der Wal,F.J., Bulleid,N.J. and High,S.
TITLE Interaction of the thiol-dependent reductase ERp57 with nascent glycoproteins
JOURNAL Science 275 (5296), 86-88 (1997)
MEDLINE 97130102
PUBMED 8974399

REFERENCE 10 (residues 1 to 505)
AUTHORS Koivunen,P., Helaakoski,T., Annunen,P., Veijola,J., Raisanen,S., Pihlajaniemi,T. and Kivirikko,K.I.
TITLE ERp60 does not substitute for protein disulphide isomerase as the beta-subunit of prolyl 4-hydroxylase
JOURNAL Biochem. J. 316 (Pt 2), 599-605 (1996)
MEDLINE 96257756
PUBMED 8687406

REFERENCE 11 (residues 1 to 505)
AUTHORS Charnock-Jones,D.S., Day,K. and Smith,S.K.
TITLE Cloning, expression and genomic organization of human placental protein disulfide isomerase (previously identified as phospholipase C alpha)
JOURNAL Int. J. Biochem. Cell Biol. 28 (1), 81-89 (1996)
MEDLINE 96191165
PUBMED 8624847

REFERENCE 12 (residues 1 to 505)
AUTHORS Hirano,N., Shibasaki,F., Sakai,R., Tanaka,T., Nishida,J., Yazaki,Y., Takenawa,T. and Hirai,H.
TITLE Molecular cloning of the human glucose-regulated protein ERp57/GRP58, a thiol-dependent reductase. Identification of its secretory form and inducible expression by the oncogenic transformation

JOURNAL Eur. J. Biochem. 234 (1), 336-342 (1995)
MEDLINE 96096758
PUBMED 8529662
REFERENCE 13 (residues 1 to 505)
AUTHORS Bourdi,M., Demady,D., Martin,J.L., Jabbour,S.K., Martin,B.M., George,J.W. and Pohl,L.R.
TITLE cDNA cloning and baculovirus expression of the human liver endoplasmic reticulum P58: characterization as a protein disulfide isomerase isoform, but not as a protease or a carnitine acyltransferase
JOURNAL Arch. Biochem. Biophys. 323 (2), 397-403 (1995)
MEDLINE 96063616
PUBMED 7487104
REFERENCE 14 (residues 1 to 505)
AUTHORS Hirano,N., Shibasaki,F., Kato,H., Sakai,R., Tanaka,T., Nishida,J., Yazaki,Y., Takenawa,T. and Hirai,H.
TITLE Molecular cloning and characterization of a cDNA for bovine phospholipase C-alpha: proposal of redesignation of phospholipase C-alpha
JOURNAL Biochem. Biophys. Res. Commun. 204 (1), 375-382 (1994)
MEDLINE 95032122
PUBMED 7945384
REFERENCE 15 (residues 1 to 505)
AUTHORS Bennett,C.F., Balcarek,J.M., Varrichio,A. and Crooke,S.T.
TITLE Molecular cloning and complete amino-acid sequence of form-I phosphoinositide-specific phospholipase C
JOURNAL Nature 334 (6179), 268-270 (1988)
MEDLINE 88288403
PUBMED 3398923
COMMENT PROVISIONAL REFSEQ: This record has not yet been subject to final NCBI review. The reference sequence was derived from BC014433.1.
On Jun 10, 2002 this sequence version replaced gi:20127473.

FEATURES Location/Qualifiers

source 1..505
/organism="Homo sapiens"
/db_xref="taxon:9606"
/chromosome="15"
/map="15q15"

Protein 1..505
/product="glucose regulated protein, 58kDa"

Region 25..133
/region_name="Thioredoxin. Thioredoxins are small enzymes that participate in redox reactions, via the reversible oxidation of an active center disulfide bond. Some members with only the active site are not separated from the noise"
/note="thiored"
/db_xref="CDD:pfam00085"

variation 41
/allele="Y"
/allele="D"
/db_xref="dbSNP:4080719"

Region 375..485
/region_name="Thioredoxin. Thioredoxins are small enzymes that participate in redox reactions, via the reversible oxidation of an active center disulfide bond. Some members with only the active site are not separated from the noise"
/note="thiored"
/db_xref="CDD:pfam00085"

variation 415
/allele="R"
/allele="K"
/db_xref="dbSNP:6413485"

```
     CDS             1..505
                     /gene="GRP58"
                     /coded_by="NM_005313.3:90..1607"
                     /note="go_component: endoplasmic reticulum [goid 0005783]
                     [evidence IEA];
                     go_function: phospholipase C activity [goid 0004629]
                     [evidence TAS] [pmid 3398923];
                     go_function: protein disulfide isomerase activity [goid
                     0003756] [evidence TAS] [pmid 8624847];
                     go_function: cysteine-type endopeptidase activity [goid
                     0004197] [evidence TAS] [pmid 9399589];
                     go_function: electron transporter activity [goid 0005489]
                     [evidence IEA];
                     go_function: isomerase activity [goid 0016853] [evidence
                     IEA];
                     go_process: protein-nucleus import [goid 0006606]
                     [evidence TAS] [pmid 7487104];
                     go_process: protein-ER retention [goid 0006621] [evidence
                     TAS] [pmid 9399589];
                     go_process: signal transduction [goid 0007165] [evidence
                     TAS] [pmid 3398923];
                     go_process: electron transport [goid 0006118] [evidence
                     IEA]"
                     /db_xref="GeneID:2923"
                     /db_xref="LocusID:2923"
                     /db_xref="MIM:602046"
ORIGIN
        1 mrlrrlalfp gvalllaaar laaasdvlel tddnfesris dtgsaglmlv effapwcghc
       61 krlapeyeaa atrlkgivpl akvdctantn tcnkygvsgy ptlkifrdge eagaydgprt
      121 adgivshlkk qagpasvplr teeefkkfis dkdasivgff ddsfseahse flkaasnlrd
      181 nyrfahtnve slvneyddng egiilfrpsh ltnkfedktv ayteqkmtsg kikkfiqeni
      241 fgicphmted nkdliqgkdl liayydvdye knakgsnywr nrvmmvakkf ldaghklnfa
      301 vasrktfshe lsdfglesta geipvvairt akgekfvmqe efsrdgkale rflqdyfdgn
      361 lkrylksepi pesndgpvkv vvaenfdeiv nnenkdvlie fyapwcghck nlepkykelg
      421 eklskdpniv iakmdatand vpspyevrgf ptiyfspank klnpkkyegg relsdfisyl
      481 qreatnppvi qeekpkkkkk aqedl
//
```

B

Eur. J. Biochem. 234, 336–342 (1995)

Molecular cloning of the human glucose-regulated protein ERp57/GRP58, a thiol-dependent reductase

Identification of its secretory form and inducible expression by the oncogenic transformation

Naoto HIRANO[1,2], Futoshi SHIBASAKI[3], Ryuichi SAKAI[2], Tomoyuki TANAKA[1,2], Junji NISHIDA[4], Yoshio YAZAKI[1], Tadaomi TAKENAWA[3] and Hisamaru HIRAI[1,2]

[1] Third Department of Internal Medicine, Faculty of Medicine, University of Tokyo, Japan
[2] Department of Molecular Biology, Jichi Medical School, Tochigi, Japan
[3] Department of Biological Research, Tokyo Metropolitan Institute of Gerontology, Japan
[4] First Department of Internal Medicine, Faculty of Medicine, Teikyo University, Tokyo, Japan

(Received 9 June 1995) – EJB 95 0928/1

Recently it was shown that putative phospholipase C-α cDNA does not code for an isotype of the phospholipase C superfamily but for one of the glucose-regulated proteins (GRPs), ERp57/GRP58. We have isolated human ERp57/GRP58 cDNA from human placenta. Sequence analysis showed that ERp57/GRP58 has two Trp-Cys-Gly-His-Cys-Lys motifs completely conserved among the mammals. Bacterially expressed recombinant ERp57/GRP58 protein contained a thiol-dependent reductase activity which was completely abolished when Ser residues were substituted for Cys residues in both of the two motifs. Furthermore, we have identified a soluble form of ERp57/GRP58 by Western blotting and biosynthetic labeling. In v-onc transformants of normal rat kidney cells, the expression level of ERp57/GRP58 was elevated at the protein level. In NIH3T3 cells transformed with v-*src*, activated c-*src* (Y527F) or c-*src*, the expression level of ERp57/GRP58 was upregulated in proportion to their transforming abilities. These results indicate that a soluble form of ERp57/GRP58 exists and that this protein may control both extracellular and intracellular redox activities through its thiol-dependent reductase activity. Moreover, it is likely that ERp57/GRP58 is involved in the oncogenic transformation.

Keywords: ERp57/GRP58; phospholipase C-α; thiol-dependent reductase; secretory protein; oncogenic transformation.

A group of stress-inducible proteins known as the glucose-regulated proteins (GRPs) are constitutively and ubiquitously expressed in mammalian cells. When the cells are deprived of glucose or treated with reagents that block protein glycosylation, perturb intracellular calcium stores, or denature proteins, the synthesis of GRPs is rapidly increased (Lee, 1987). GRP94 and GRP78 are major members of this family and are abundant proteins in the luminal endoplasmic reticulum (ER) acting as 'molecular chaperons'. GRP78 and GRP94 share sequence similarity with the heat shock protein 70 and the heat shock protein 90, respectively (Gething and Sambrook, 1992). In the capacity of a molecular chaperone protein, GRP78 and GRP94 transiently bind to a wide repertoire of proteins traversing through the ER and facilitate their folding, assembly, and transport (Hendershot, 1990; Melnick et al., 1992).

Correspondence to H. Hirai, Third Department of Internal Medicine, Faculty of Medicine, University of Tokyo, 7-3-1 Hongo, Bunkyo-ku, Tokyo, Japan 113
Fax: +81 3 3815 8350.

Abbreviations. DMEM, Dulbecco's modified Eagle's medium; ER, endoplasmic reticulum; GRP, glucose-regulated protein; GST, glutathione *S*-transferase; NRK, normal rat kidney; PDI, protein disulfide-isomerase; PLC, phospholipase C.

Enzymes. Phospholipase C (EC 3.1.4.3); protein disulfide-isomerase (EC 5.3.4.1); protein-disulfide reductase (EC 1.8.4.2).

Note. The nucleotide sequence data reported in this paper have been submitted to the DDBJ/GenBank/EMBL nucleotide sequence database and are available under accession number D16235.

Another member of the family, GRP58, was first discovered in a temperature-sensitive hamster fibroblast line K12 as a 58-kDa protein with a pI of 5.9 (Lee, 1981; Melero and Smith, 1978). However, cDNA encoding GRP58 was never cloned and the function of GRP58 has remained obscure. Very recently, it was reported that GRP58 is identical to putative phospholipase C-α (PLC-α) (Mazzarella et al., 1994). PLC-α cDNA was initially cloned from guinea pig uterus by expression cloning with polyclonal antibody raised against the purified protein which had PLC activity (Bennett et al., 1988). We and others, however, showed that PLC-α cDNA does not encode any functional PLC activity and we redesignated it ERp57 (Hirano et al., 1994; Martin et al., 1991; Srivastava et al., 1993). Moreover, it was revealed that PLC-α contains thiol-group-related proteolytic activity, and protein disulfide-isomerase activity (Srivastava et al., 1993; Urade et al., 1992). It is now concluded that putative PLC-α cDNA encodes ERp57/GRP58 and not a member of the PLC family.

Rat, mouse, and bovine ERp57/GRP58 proteins contain a characteristic 110-amino-acid sequence which is repeated twice within the protein sequence. In each repeat a Trp-Cys-Gly-His-Cys-Lys motif exists, which is identical to the active sites of protein disulfide-isomerase (PDI) and ERp72 and is highly similar to that of thioredoxin. PDI catalyzes protein disulfide formation, reduction, and isomerization *in vitro*, depending on the reaction conditions, and is regarded as the *in vivo* catalyst of disulfide bond formation in the synthesis of various secretory pro-

teins (Freedman, 1989). The predicted amino acid sequence contains two Trp-Cys-Gly-His-Cys-Lys motifs which act as catalytic sites for the isomerase activity. ERp72 is another abundant luminal ER protein and has been identified as a novel relative of PDI. Murine ERp72 contains three copies of the Trp-Cys-Gly-His-Cys-Lys motif with a spacing between two copies which is nearly identical to that found in PDI (Mazzarella et al., 1990). The cellular role of ERp72 has been little understood. Several lines of evidence support the idea that PDI and ERp72 should both function as a molecular chaperone (Kuznetsov et al., 1994; Nigam et al., 1994). Thioredoxin has been isolated from a wide variety of prokaryotic and eukaryotic species. It contains protein-disulfide-isomerase and protein-disulfide reductase activities with a single active site, the Trp-Cys-Gly-Pro-Cys-Lys motif.

Previously we cloned and characterized bovine ERp57/GRP58 cDNA (Hirano et al., 1994). In this paper, we describe the isolation of human ERp57/GRP58 cDNA from human placenta. Sequence analysis showed that ERp57/GRP58 is highly conserved among mammals. Bacterially expressed and purified recombinant ERp57/GRP58 protein possessed a thiol-dependent reductase activity. Furthermore, we have detected a secretion of ERp57/GRP58 protein in cultured medium by immunoblotting and biosynthetic labeling. We also provide evidence that ERp57/GRP58 is involved in oncogenic transformation.

MATERIALS AND METHODS

Cloning of human ERp57/GRP58 cDNA. In order to obtain human ERp57/GRP58 cDNA, 5×10^4 of recombinant phages from a λZAPII human placental cDNA library (gift from H. Toyoshima) were screened with the ^{32}P-labeled full-length bovine ERp57/GRP58 cDNA under low stringent condition. The single positive clone was isolated and the cloned 1.9-kb insert was excised *in vivo* (Sambrook et al., 1989). Nested deletions were generated using the Exo-Mung deletion kit (Pharmacia). Double-stranded DNA was sequenced using the Sequenase 2.0 system (United States Biochemical) on both strands.

Cell lines and immunoblotting. F02 and R06 are NIH3T3-derived sublines stably transfected with a sense construct and an antisense construct of bovine ERp57/GRP58 cDNA, respectively (Hirano et al., 1994). Sublines derived from normal rat kidney were gifts from H. Okayama. NIH3T3-derived *src*-transfectants have been described elsewhere (Hirai and Varmus, 1990).

To collect total cell lysates, cells were grown up to the confluent state and lysed on ice in lysis buffer L containing, 50 mM Tris/HCl pH 7.4, 150 mM NaCl, 0.05% (mass/vol.) sodium dodecyl sulfate, 1% sodium deoxycholate, 1% (by vol.) Triton X-100, 10 U/ml aprotinin, 2 mM phenylmethylsulfonyl fluoride, 100 mg/l leupeptin, 1 mM sodium orthovanadate. Insoluble materials were removed by centrifugation. Protein concentration was determined with a protein assay kit (Bio-Rad) and equal amounts of cell lysates were separated by SDS/PAGE. To collect supernatants, cells were grown up to a semiconfluent state in 150-mm dishes in Dulbecco's modified Eagle's medium (DMEM) with 10% bovine serum and washed with phosphate-buffered saline. Then cells were incubated in 20 ml serum-free medium (Cell Grosser P, Sumitomo Pharmaceutical). After 10 h, supernatants were collected, centrifuged, and dialyzed against water. Dialyzed supernatants were lyophilized and analyzed on SDS/PAGE. Separated proteins were electrophoretically transferred to Immobilon-P membrane filters (Millipore). The filters were blocked for 3 h in buffer A (10 mM Tris/HCl pH 8.0, 150 mM NaCl, 0.5% Tween 20), and 1% bovine serum albumin (fraction V, Boehringer-Manheim) and incubated for 1 h with anti-ERp57/GRP58 serum (Hirano et al., 1994) or anti-Grb2/Ash antibody (MBL) in buffer A. Anti-ERp57/GRP58 serum recognizes bovine, mouse, rat, and human ERp57/GRP58 proteins with immunoblotting. The filters were then washed three times with buffer A and incubated with alkaline-phosphatase-conjugated second antibody for 1 h. Color was developed according to the manufacturer's instruction (Promega).

Bacterial expression of wild and mutant ERp57/GRP58 proteins. Partial bovine ERp57/GRP58 cDNA (encoding amino acid residues 27–505) was blunt-ended with mung bean nuclease and subcloned in frame into the *Sma*I site of pGEX2T bacterial expression vector (Pharmacia) to generate pGEX-ERp57/GRP58 plasmid. An overnight culture of *Escherichia coli* XL-1B (pGEX-ERp57/GRP58) was diluted 1:10 (with 100 mg ampicillin/ml), grown for 18 h at 25°C, and induced for another 6 h by addition of isopropyl β-D-thiogalactoside to 0.1 mM. Bacteria were lysed by freeze/thaw in lysis buffer containing 50 mM Tris/HCl pH 7.5, 25% sucrose, 0.5% Nonidet P-40, 5 mM $MgCl_2$. Lysates were cleared by centrifugation. Supernatants were filtrated through 1.2-μm Acrodiscs (Gelman-Sciences) and applied to a column of glutathione–Sepharose 4B (Pharmacia). The column was washed with wash buffer containing 20 mM Tris/HCl pH 7.5, 2 mM $MgCl_2$, 1 mM dithiothreitol, and then eluted with elution buffer containing 5 mM glutathione, 50 mM Tris/HCl pH 9.5. Eluates were collected in 1.5-ml fractions and analyzed by SDS/PAGE. Fractions including the fusion protein between glutathione *S*-transferase (GST) and ERp57/GRP58 were collected and dialyzed intensively against dialysis buffer containing 20 mM Tris/HCl pH 7.5, 10 mM dithiothreitol. Dialyzed fractions were then incubated at room temperature for 1.5 h in digestion buffer containing 2.5 mM $CaCl_2$, 50 mM Tris/HCl pH 7.5, 150 mM NaCl and 400 U human thrombin (Sigma)/mg fusion protein. Resultant recombinant ERp57/GRP58 protein includes only two amino acid residues of GST at the N-terminus. Contaminating proteins, mainly GST, were removed by FPLC on a Superdex 16/60 column (Pharmacia). Purified ERp57/GRP58 protein was intensively dialyzed against water and lyophilized.

The *dut*$^-$ *ung*$^-$ bacterial strain CJ236 and protocols from the Muta-Gene kit (Bio-Rad) were used to generate oligonucleotide-directed mutations in the Trp-Cys-Gly-His-Cys-Lys motifs. Partial bovine ERp57/GRP58 cDNA (encoding amino acid residues 27–505) was subcloned into M13mp18, and mutagenesis was performed on uracil-substituted viral DNA. Mutant *Eco*RI fragment was excised from M13 replicative-form DNA, blunt-ended with mung bean nuclease, and reinserted into pGEX2T generating pGEX-mut-ERp57/GRP58. The mutagenic primer 5′-GCCCCCTGGTCTCCACACAGCAAAAAGCTT-3′ (sense) changes Cys57 and Cys60 to Ser while 5′-GCTCCTTGGTCTGGTCACTCTAAGAATCTG-3′ (sense) changes Cys406 and Cys409 to Ser. The resulting mutant was sequenced to verify the sequence.

Insulin turbidity assay. Freshly prepared solutions of insulin, 1 mg/ml in 100 mM potassium acetate pH 7.5, 2 mM EDTA, and 10 μM dithiothreitol were stored on ice. The assay mixture was prepared in a cuvette by addition of 50 μl insulin plus the tested protein and water to give a final volume of 60 μl. The reaction was started by pipetting 2 μl dithiothreitol in a cuvette. The cuvette was then thoroughly mixed and placed in the spectrophotometer. The measurements were performed at 650 nm using 80-s recordings. Assays lasting up to 80 min were not mixed further. The nonenzymic reduction of insulin by dithiothreitol was recorded as a control. *E. coli* thioredoxin was purchased from Promega and used as a positive control.

Biosynthetic labeling of ERp57/GRP58. 6×10^4 F02 and R06 cells/well were seeded onto a 24-well plate and cultured in DMEM containing 10% bovine serum. The next day medium

were removed and washed with methionine-free DMEM. Then cells were labeled with 0.5 mCi [^{35}S]methione in 300 µl methionine-free DMEM with 1% bovine serum for 16 h at 37°C. Cells were lysed in lysis buffer L (see above). Cultured medium was centrifuged at 100000 *g* for 1 h at 4°C and the supernatants were carefully collected. Radiolabeled cells and supernatants were collected separately. Cell lysates and supernatants were subjected to 9% SDS/PAGE, and then autoradiographed.

RESULTS

Cloning of human ERp57/GRP58 cDNA. In order to obtain human cDNA of ERp57/GRP58, a human placental cDNA library was screened with bovine ERp57/GRP58 cDNA under low stringent conditions. The single positive clone was isolated and completely sequenced (Fig. 1). Human ERp57/GRP58 cDNA consists of a 1515-bp open-reading frame predicting a polypeptide of 505 amino acids with a calculated molecular mass of 56698 Da. It contains a polyadenylation signal (AATAAA) 16 bp upstream of the poly(A) tail and hydrophobic N-terminal signal peptides (amino acid residues 1−24) predicted by the method of von Heijne (1986).

The deduced amino acid sequence exhibits an overall identity of 90%, 87%, and 94% to that of murine (Hempel and DeFranco, 1991), rat (Bennett et al., 1988), and bovine ERp57/GRP58 (Hirano et al., 1994), respectively (Fig. 2). Human ERp57/GRP58 has 56% amino acid similarity and 32% identity overall with human PDI (Pihlajaniemi et al., 1987). Amino acid positions 25−129 of human ERp57/GRP58 exhibit 55% similarity and 23% identity overall with human thioredoxin (Tagaya et al., 1989). ERp57/GRP58 and PDI contain two and ERp72 contains three copies of the Trp-Cys-Gly-His-Cys-Lys motif which is highly similar to the Trp-Cys-Gly-Pro-Cys-Lys motif of thioredoxin.

Purification of bacterially expressed ERp57/GRP58. To generate recombinant ERp57/GRP58 protein, we utilized the GEX *E. coli* expression system. Initially, the full-length bovine ERp57/GRP58 cDNA was fused downstream of the glutathione *S*-transferase (GST) gene in the pGEX2T expression vector, and the fusion protein was induced with isopropyl thiogalactoside. However, the protein was hardly soluble and was not adequate for the following purification. Therefore, partial bovine ERp57/GRP58 cDNA, encoding amino acids 27−505 (the signal peptide and the following two amino acid residues were removed), was subcloned into pGEX2T and the GST-ERp57/GRP58 fusion protein was induced with isopropyl thiogalactoside. The fusion protein was purified on a glutathione−Sepharose column and digested with thrombin in order to remove the GST moiety. Then the proteins were purified with gel filtration and bacterially expressed ERp57/GRP58 protein was obtained (Fig. 3).

ERp57/GRP58 has thiol-dependent reductase activity which catalyzes the reduction of insulin disulfides by dithiothreitol. Both PDI and thioredoxin are multifunctional proteins that can catalyze thiol/disulfide exchange reactions acting as protein-disulfide reductase and protein disulfide-isomerase. The two conserved Trp-Cys-Gly-His-Cys-Lys motifs of mammalian PDI and the single similar motif, Trp-Cys-Gly-Pro-Cys-Lys, of all the thioredoxins of prokaryotes and eukaryotes, are thought to be the active sites for their catalytic activities. Since mammalian ERp57/GRP58 contains two conserved motifs completely identical to those of PDI, we presumed that ERp57/GRP58 has a similar reducing activity. Reduction of insulin leads to cleavage of the two interchain disulfide bridges and formation of a white

```
1     GGCGCCGACCTCCGCAGTCCCAGCCGAGCCGCGACCCTTCCGGCCGTCCC
51    CACCCCACCTCGCCGCCATGCGCCTCCGCCGCCTAGCGCTGTTCCCGGGT
                    M  R  L  R  R  L  A  L  F  P  G
101   GTGGCGCTGCTTCTTGCCGCGGCCCGGCCTCGCCGCTGCCTCCGACGTGCT
      V  A  L  L  L  A  A  A  R  L  A  A  A  S  D  V  L
151   AGAACTCACGGACGACAACTTCGAGAGTCGCATCTCCGACACGGGCTCTG
      E  L  T  D  D  N  F  E  S  R  I  S  D  T  G  S  A
201   CGGGCCTCATGCTCGTCGAGTTCTTCGCTCCCTGGTGTGGACACTGCAAG
      G  L  M  L  V  E  F  F  A  P  W  C  G  H  C  K
251   AGACTTGCACCTGAGTATGAAGCTGCAGCTACCAGATTAAAAGGAATAGT
      R  L  A  P  E  Y  E  A  A  A  T  R  L  K  G  I  V
301   CCCATTAGCAAAGGTTGATTGCACTGCCAACACTAACACCTGTAATAAAT
      P  L  A  K  V  D  C  T  A  N  T  N  T  C  N  K  Y
351   ATGGAGTCAGTGGATATCCAACCCTGAAGATATTTAGAGATGGTGAAGAA
      G  V  S  G  Y  P  T  L  K  I  F  R  D  G  E  E
401   GCAGGTGCTTATGATGGACCTAGGACTGCTGATGGAATTGTCAGCCACTT
      A  G  A  Y  D  G  P  R  T  A  D  G  I  V  S  H  L
451   GAAGAAGCAGGCAGGACCAGCTTCAGTGCCTCTCAGGACTGAGGAAGAAT
      K  K  Q  A  G  P  A  S  V  P  L  R  T  E  E  E  F
501   TTAAGAAATTCATTAGTGATAAAGATGCCTCTATAGTAGGTTTTTTCGAT
      K  K  F  I  S  D  K  D  A  S  I  V  G  F  F  D
551   GATTCATTCAGTGAGGCTCACTCCGAGTTCCTAAAAGCAGCCAGCAACTT
      D  S  F  S  E  A  H  S  E  F  L  K  A  A  S  N  L
601   GAGGGATAACTACCGATTTGCACATACGAATGTTGAGTCTCTGGTGAACG
      R  D  N  Y  R  F  A  H  T  N  V  E  S  L  V  N  E
651   AGTATGATGATAATGGAGAGGGTATCATCTTATTTCGTCCTTCACATCTC
      Y  D  D  N  G  E  G  I  I  L  F  R  P  S  H  L
701   ACTAACAAGTTTGAGTACAAGACTGTGGCATATACAGAGCAAAAAATGAC
      T  N  K  F  E  Y  K  T  V  A  Y  T  E  Q  K  M  T
751   CAGTGGCAAAATTAAAAAGTTTATCCAGGAAAACATTTTTGGTATCTGCC
      S  G  K  I  K  K  F  I  Q  E  N  I  F  G  I  C  P
801   CTCACATGACAGAGGACAATAAAGATTTGATACAGGGCAAGGACTTACTT
      H  M  T  E  D  N  K  D  L  I  Q  G  K  D  L  L
851   ATTGCTTACTATGATGTGGACTATGAAAAGGACGCTAAAGGTTCCAACTA
      I  A  Y  Y  D  V  D  Y  E  K  D  A  K  G  S  N  Y
901   CTGGAGAAACAGGGTAATGATGGTGGCAAAGAAATTCCTGGATGCTGGGC
      W  R  N  R  V  M  M  V  A  K  K  F  L  D  A  G  H
951   ACAAACTCAACTTTGCTGTAGCTAGCCGCAAAACCTTTAGCCATGAACTT
      K  L  N  F  A  V  A  S  R  K  T  F  S  H  E  L
1001  TCTGATTTTGGCTTGGAGAGCACTGCTGGAGAGATTCCTGTTGTTGCTAT
      S  D  F  G  L  E  S  T  A  G  E  I  P  V  V  A  I
1051  CAGGACTGCTAAAGGAGAGAAGTTTGTCATGCAGGAGGAGTTCTCGCGTG
      R  T  A  K  G  E  K  F  V  M  Q  E  E  F  S  R  D
1101  ATGGGAAGGCTCTGGAGAGGTTCCTGCAGGGTTACTTTGGTGGCAATCTG
      G  K  A  L  E  R  F  L  Q  G  Y  F  G  G  N  L
1151  AAGAGATACCTGAAGTCTGACCCTATCCCAGAGAGCAATGATGGGCCTGT
      K  R  Y  L  K  S  D  P  I  P  E  S  N  D  G  P  V
1201  GAAGGTAGTGGTAGCAGAGAATTTTGATGAAATAGTGAATAATGAAAATA
      K  V  V  V  A  E  N  F  D  E  I  V  N  N  E  N  K
1251  AAGATGTGCTGATTGAATTTTATGCCCCTTGGTGTGGTCATTGTAAGAAC
      D  V  L  I  E  F  Y  A  P  W  C  G  H  C  K  N
1301  CTGGAGCCCAAGTATAAAGAACTTGGCGAGAAGCTCAGCAAAGACCCAAA
      L  E  P  K  Y  K  E  L  G  E  K  L  S  K  D  P  N
1351  TATCGTCATAGCCAAGATGGATGCCACAGCCAATGATGTGCCTTCTCCAT
      I  V  I  A  K  M  D  A  T  A  N  D  V  P  S  P  Y
1401  ATGAAGTCAGAGGTTTTCCTACCATATACTTCTCTCCAGCCAACAAGAAG
      E  V  R  G  F  P  T  I  Y  F  S  P  A  N  K  K
1451  CTAAATCCAAAGAAATATGAAGGTGGCCGTGAATTAAGTGATTTTATTAG
      L  N  F  K  K  Y  E  G  G  R  E  L  S  D  F  I  S
1501  CTATCTACAAAGAGAAGCTACAAACCCCCCTGTAATTCAAGAAGAAAAAC
      Y  L  Q  R  E  A  T  N  P  P  V  I  Q  E  E  K  P
1551  CCAAGAAGAAGAAGAAGGCACAGGAGGATCTCTAAAGCAGTAGCCAAACA
      K  K  K  K  K  A  Q  E  D  L
1601  CCACTTTGTAAAAGGACTCTTCCATCAGAGATGGAAAACCATTGGGGAGG
1651  GACTAGGACCCATATGGGAATTATTACCTCTCAGGGCCGAGAGGACAGAA
1701  TGGAAATAATCTGAATCCTGTTAAATTTTCTCTAAACTGTTTCTTAGCTG
1751  CACTGTTTATGGAAATACCAGGAACCAGTTTATGTTTGTGGTTTTGGGAA
1801  AAATTATTTGTGTTGGGGGAAATGTTGTGGGGGTGGGGTTGAGTTGGGGG
1851  ATATTTTCTAATTTTTTTTGTACATTTGGAACAGTGACCAATAAATGAGA
1901  CCCCTTTAAACTGTCAAAAAAAAAAAAAAAAAA
```

Fig. 1. The nucleotide and deduced amino acid sequences of human ERp57/GRP58 cDNA. The deduced amino acid sequence is shown in the one-letter code. The polyadenylation signal is underlined.

insoluble precipitate from the free α and β chains, mainly from the β chain of insulin (Srinivasan et al., 1975). This phenomenon enabled us to measure protein disulfide reduction directly with a spectrophotomeric assay that records the turbidity of precipitation at 650 nm (Holmgren, 1979). Using this standard assay system, we tested the reducing activity of ERp57/GRP58 on insulin with dithiothreitol, and compared it with that of thioredoxin. The reduction of insulin disulfides by dithiothreitol was determined in the presence or absence of recombinant ERp57/GRP58 protein. The assay mixtures contained a final concentration o

```
bovine  MRLRRLALFPGLALLLAAARLAAASDVLELTDDNFESRITDTGSSGLIVV
human   MRLRRLALFPGVALLLAAARLAAASDVLELTDDNFESRISDTGSAGLMLV
mouse   MRFSCLALLPGVALLLASARLAAASDVLELTDENFESRVSDTGSAGLMLV
rat     MPSAALRCSRAWRLLLASALLASASDVLELTDENFESRVSDTGSAGLMLV

bovine  EFFAPWCGHCKRLAPEYEAAATRLKGIVPLAKVDCTANTNTCNKYGVSGY
human   EFFAPWCGHCKRLAPEYEAAATRLKGIVPLAKVDCTANTNTCNKYGVSGY
mouse   EFFAPWCGHCKRLAPEYEAAATRLK-IVPLAKVDCTANTNTCNKYGVSGY
rat     EFFAPWCGHCKRLAPEYEAAATRLKGIVPLAKVDCTANTNTCNKYGVTGY

bovine  PTLKIFRDGEESGAYDGPRTADGIVSHLKKQAGPASVPLKSEEEFEKFIS
human   PTLKIFRDGEEAGAYDGPRTADGIVSHLKKQAGPASVPLRTEEEFKKFIS
mouse   PTLKIFRAGEEAGAYDGPRTADGIVSHLKKQAGPASVPLRTEEEFKKFIS
rat     PTLKIFRDGEEAGAYDGPRTADGIVSHLKKQAGPASVPLRTEDEFKKFIS

bovine  DKDASVVGFFKDLFSEAHSEFLKAASNLRDNYRFAHTNVESLVNKYDDDG
human   DKDASIVGFFDDSFSEAHSEFLKAASNLRDNYRFAHTNVESLVNEYDDNG
mouse   DKDASVVGFFRDLFSDGHSEFLKAASNLRDNYRFAHTNIESLVKEYDDNG
rat     DKDASVVGFFRDLFSDGHSEFLKAASNLRDNYRFAHTNVESLVKEYDDNG

bovine  EGITLFRPSHLTNKFEDKTVAYTEQKMTSGKIKRFIQENIFGICPHMTED
human   EGIILFRPSHLTNKFEYKTVAYTEQKMTSGKIKKFIQENIFGICPHMTED
mouse   EGITIFRPLHLANKFEDKTVAYTEKKMTSAKIKKFIQDSIFGLCPHMTED
rat     EGITIFRPLHLANKFEDKIVAYTEKKMTSGKSRSLFRKA-FGLCPHMTED

bovine  NKDLLQGKDLLIAYYDVDYEKNAKGSNYWRNRVMMVAKKFLDAGQKLHFA
human   NKDLIQGKDLLIAYYDVDYEKDAKGSNYWRNRVMMVAKKFLDAGHKLNFA
mouse   NKDLIQGKDLLTAYYDVDYEKNAKGSNYWRNRVMMVAKKFLDAGHKLNFA
rat     NKDLIQGKDLLTAYYDVDYEKNTKGSNYWRNRVMMVAKTFLDAGHKLNFA

bovine  VASRKTFSHELSDFGLESTTGEIPVVAVRTAKGEKFVMQEEFSRDGKALE
human   VASRKTFSHELSDFGLESTAGEIPVVAIRTAKGEKFVMQEEFSRDGKALE
mouse   VASRKTFSHELSDFSLESTTGEVPVVAIRTAKGEKFVMQEEFSRDGKALE
rat     VASRKTFSHELSDFGLESTTGEIPVVAIRTAKGEKFVMQEEFSRDGKALE

bovine  RFLEDYFDGNLKRYLKSEPIPESNDGPVKVVVAENFDEIVNNENKDVLIE
human   RFLQGYFGGNLKRYLKSDPIPESNDGPVKVVVAENFDEIVNNENKDVLIE
mouse   QFLQEYFDGNLKRYLKSEPIPESNEGPVKVVVAENFDDIVNEEDKDVLIE
rat     RFLQEYFDGNLKRYLKSEPIPETNEGPVKVVVAESFDDIVNAEDKDVLIE

bovine  FYAPWCGHCKNLEPKYKELGEKLRKDPNIVIAKMDATANDVPSPYEVRGF
human   FYAPWCGHCKNLEPKYKELGEKLSKDPNIVIAKMDATANDVPSPYEVRGF
mouse   FYAPWCGHCKNLEPKYKELGEKLSKDPNIVIAKMDATANDVPSPYEVKGF
rat     FYAPWCGHCKNLEPKYKELGEKLSKDPNIVIAKMDATANDVPSPYEVKGF

bovine  PTIYFSPANKKQNPKKYEGGRELSDFISYLKREATNPPVIQEEKPKKKKK
human   PTIYFSPANKKLNPKKYEGGRELSDFISYLQREATNPPVIQEEKPKKKKK
mouse   PTIYFSPANKKLTPKKYEGGRELNDFISYLQREATNPPIIQEEKPKKKKK
rat     PTIYFSPANKKLTPKKYEGGRELNDFISYLQREATNPPIIQEEKPKKKKK

bovine  ADEDL
human   ADEDL
mouse   ADEDL
rat     ADEDL
```

Fig. 2. Amino acid sequence comparison of bovine, human, rat, and mouse ERp57/GRP58. Amino-terminal hydrophobic stretches predicted to be signal peptides are underlined. The conserved motifs, Trp-Cys-Gly-His-Cys-Lys, and ER-retention signal-like sequences are boxed. Asterisks and dots below the alignment indicate identical residues and conservative replacements, respectively. Dashes indicate gaps introduced for optimal alignment.

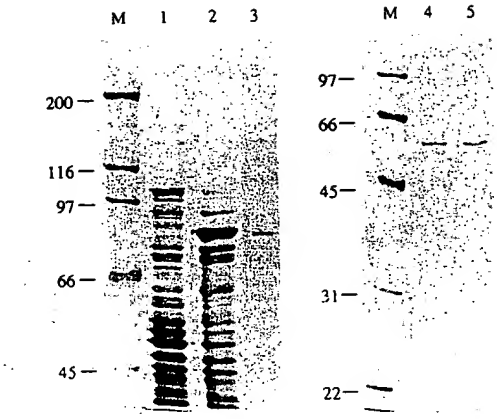

Fig. 3. SDS/PAGE illustrating the purification of ERp57/GRP58 protein expressed in *E. coli* and visualized with Coomassie blue staining. Protein samples after each purification step were run on a SDS/polyacrylamide gel. Lane 1, lysates of *E. coli* (pGEX-ERp57/GRP58), not induced with isopropyl thiogalactoside; lane 2, lysates of *E. coli* (pGEX-ERp57/GRP58) induced with isopropyl thiogalactoside; lane 3, GST-ERp57/GRP58; lane 4, wild-type ERp57/GRP58; lane 5, mutant ERp57/GRP58; M, molecular mass standards with values given in kDa.

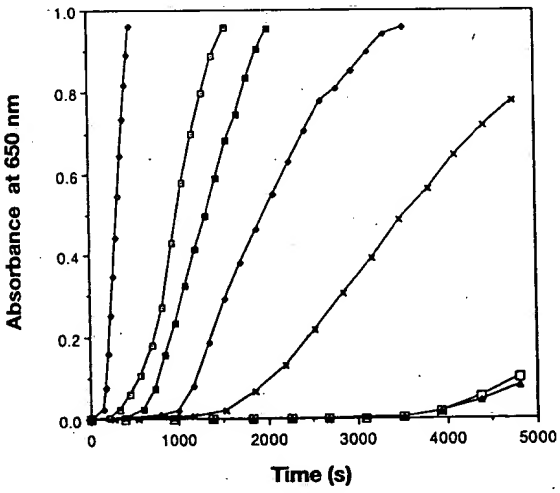

Fig. 4. Thiol-dependent catalytic activity of ERp57/GRP58 protein assayed with the insulin precipitation method. The assay mixture was prepared in a cuvette by addition of 50 µl insulin plus tested protein and water to give a final volume of 60 µl. The reaction was started by pipetting 2 µl 10 mM dithiothreitol in a cuvette; the absorbance at 650 nm is plotted against time. Dithiothreitol alone, without thioredoxin or ERp57/GRP58, served as control (▲). (□) 8.4 µM and (◆) 4.2 µM ERp57/GRP58; (◇) 19.0 µM, (■) 3.8 µM and (×) 0.8 µM thioredoxin.

0.13 mM insulin and 0.33 mM dithiothreitol. In the control cuvette containing only dithiothreitol, no precipitation was observed within 60 min. The addition of 8.4 µM ERp57/GRP58 resulted in rapid precipitation appearing after 6 min, showing a catalytic effect of ERp57/GRP58 protein, while 4.2 µM ERp57/GRP58 resulted in a longer delay before turbidity emerged and a slower rate of precipitation. The addition of 3.8 µM thioredoxin brought nearly the same precipitation delay and rate, suggesting that, on a the molar basis, thioredoxin could be two–three times as effective as ERp57/GRP58 (Fig. 4). After leaving the assay cuvettes overnight, nearly the same amount of precipitate was observed irrespective of the amount of ERp57/GRP58 or thioredoxin (data not shown).

Since the disulfide bond formed by vicinal Cys residues in the sequence Trp-Cys-Gly-His/Pro-Cys-Lys is thought to be the redox active site in PDI or thioredoxin, we examined whether vicinal Cys residues in the two Trp-Cys-Gly-His-Cys-Lys motifs of ERp57/GRP58 are the active sites for the reductase activity or not. Oligonucleotide-directed mutagenesis was used to create two amino acid substitutions, Trp-Ser-Gly-His-Ser-Lys, in both of the two motifs of ERp57/GRP58. Utilizing the GEX system, we bacterially expressed and purified mutant ERp57/GRP58 protein (Fig. 3, lane 5). We assayed insulin precipitation with the mutant ERp57/GRP58 protein but it was unable to accelerate precipitation of insulin at all, unlike wild-type ERp57/GRP58 protein (Fig. 4). These results clearly demonstrate that ERp57/GRP58 is capable of catalyzing reduction of disulfides and that the two vicinal Cys residues in the Trp-Cys-Gly-His-Cys-Lys motif are responsible for the reductase activity.

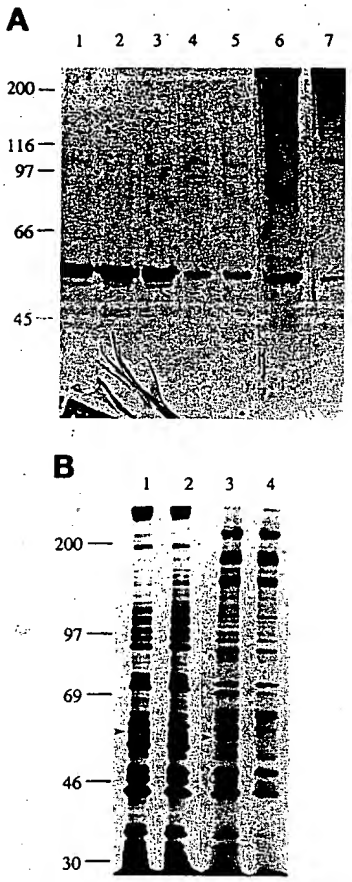

Fig. 5. Expression of ERp57/GRP58 in total cell lysates and supernatants of NIH3T3 sublines transfected with ERp57/GRP58 cDNA. F01, F02, F03 are independent NIH3T3 sublines transfected with a sense construct. R01 and R06 are independent cell lines transfected with an antisense construct (Hirano et al., 1994). (A) Immunoblot analysis of ERp57/GRP58 in the total cell lysates (lanes 1–5) and supernatants (lanes 6 and 7) of F01 (lane 1), F02 (lanes 2 and 6) F03 (lane 3), R01 (lane 4), and R06 (lanes 5 and 7). Equal amounts (100 μg) of cell lysates and supernatants were separated by SDS/PAGE and probed with anti-ERp57/GRP58. (B) Biosynthetic labeling of ERp57/GRP58. F02 and R06 cells in the total cell lysates (lanes 1 and 2) and supernatants (lanes 3 and 4) of F02 (lanes 1 and 3) and R06 (lanes 2 and 4) cells. Cells were labeled with 0.5 mCi [^{35}S]methione, lysed in lysis buffer L. Supernatants were collected separately. Cell lysates and supernatants were subjected to SDS/PAGE, and then autoradiographed. Positions of molecular mass markers are indicated.

Soluble form of ERp57/GRP58. Mammalian ERp57/GRP58 is predicted to have a signal peptide sequence at the N-terminus and an ER-retention signal-like sequence, Gln-Glu-Asp-Leu at the C-terminus (Fig. 2). The C-terminal sequence of PDI, Lys-Asp-Glu-Leu, and that of ERp72, Lys-Glu-Glu-Leu, are retention signals for their respective proteins. Mutant PDI or ERp72 with the C-terminal Gln-Glu-Asp-Leu sequence, however, was secreted and retention efficiency decreased to the point where the level of secretion approached that of the mutants without native retention signal sequences (Haugejörden et al., 1991). Thus, we examined whether a soluble form of ERp57/GRP58 exists in culture medium. F02 and R06 are NIH3T3-derived sublines stably transfected with a sense construct and an antisense construct of bovine ERp57/GRP58 cDNA, respectively (Hirano et al., 1994). The supernatants of F02 and R06 cells were subjected to SDS/PAGE and immunoblotted with anti-ERp57/GRP58 serum. F02 cells transfected with the sense ERp57/GRP58 construct produced a substantial amount of ERp57/GRP58 in the culture medium, while the supernatant of R06 cells transfected with the antisense construct showed only a marginal band (Fig. 5A). This indicates that ERp57/GRP58 is a secretory protein and that the parental NIH3T3 cell produces endogenous mouse ERp57/GRP58 into culture medium. We have also confirmed the secretion of ERp57/GRP58 by biosynthetic labeling. Total lysates and supernatants from *in vivo* labeled F02 and R06 cell lines were collected and analyzed on SDS/PAGE. The soluble form of ERp57/GRP58 was detected in both the lysates and supernatants of F02 cells but not of R06 cells (Fig. 5B). There was no indication of cell breakage during the serum-free incubation or *in vivo* labeling of cells. These results clearly demonstrate that the Gln-Glu-Asp-Leu sequence at the C-terminus of ERp57/GRP58 does not fully function as an ER-retention signal sequence.

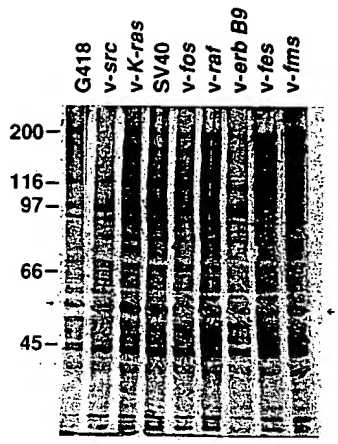

Fig. 6. Induction of ERp57/GRP58 by oncogenic transformation in NRK cells. NRK cells were transfected with each individual v-onc gene and G418-selected. Equal amounts (100 μg) of cell lysates of NRK-derived cells were separated by SDS/PAGE and probed with anti-ERp57/GRP58 serum. Positions of molecular mass markers are indicated.

Expression level of ERp57/GRP58 in transformed cells. We investigated the expression level of ERp57/GRP58 by Western analysis in normal rat kidney (NRK) cells transformed by various kinds of oncogenes. Total lysates from subconfluent NRK-derived cells were collected and immunoblotted with anti-ERp57/GRP58 serum. As shown in Fig. 6, the protein level of ERp57/GRP58 was increased in all NRK-derived transformants. In NRK cells transformed with v-*src*, v-*K-ras* or simian virus 40 ERp57/GRP58 expression was induced 7–8-fold compared with that of G418-selected NRK cells. The ERp57/GRP58 expression was enhanced 3–4-fold in v-*fos*, v-*raf*, v-*erb B9*, and v-*fes* transformants. These results indicate that the expression of ERp57/GRP58 is induced by the oncogenic transformation of NRK cells.

In order to address the relationship between the transforming abilities and the expression level of ERp57/GRP58, we examined NIH3T3 cells transfected with normal c-*src*, activated c-*src* (Y527F), and v-*src*. The ERp57/GRP58 protein levels in NIH3T3 cells transfected with v-*src* and activated c-*src* (Y527F) were about seven and three times as much as that in non-transfected NIH3T3 cells, respectively. On the other hand, the expression level of ERp57/GRP58 in c-*src*-transfected cells was as much as that in G418-selected NIH3T3 cells (Fig. 7). These data show that the expression level of ERp57/GRP58 is upregulated in proportion to the transforming abilities. Southern blot analysis revealed that there is no rearrangement or amplification of the ERp57/GRP58 gene in *src*-transfected NIH3T3 cells (data

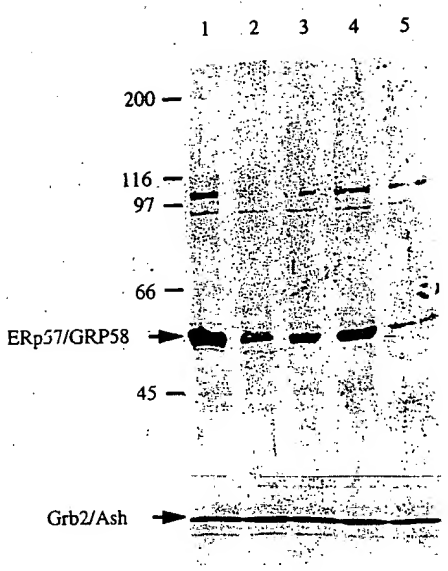

Fig. 7. The ERp57/GRP58 expression is upregulated in proportion to the *src*-transforming abilities. NIH3T3 cells were transfected with each individual *src* gene and G418-selected. Equal amounts (100 μg) of cell lysates of NIH3T3-derived F02 (lane 1), c-*src* (lane 2), activated c-*src* (Y527F) (lane 3), v-*src* (lane 4) transfectants and parental NIH3T3 cells (lane 5) were separated by SDS/PAGE and probed with anti-ERp57/GRP58 serum. Expression of Grb2/Ash served as an internal control for the amount of protein loaded in each lane. Positions of molecular mass markers are indicated.

not shown); *src* expression levels were comparable in *src*-transfected cells (Hirai and Varmus, 1990).

DISCUSSION

In this paper we describe the isolation of human ERp57/GRP58 cDNA from human placenta. Mammalian ERp57/GRP58 proteins share two copies of the Trp-Cys-Gly-His-Cys-Lys motif that is found in PDI and ERp72 and which is highly similar to the motif Trp-Cys-Gly-Pro-Cys-Lys found in thioredoxin. Either PDI or thioredoxin contains protein disulfide-isomerase and protein-disulfide reductase activities, whose active sites are thought to be the Trp-Cys-Gly-His/Pro-Cys-Lys motifs. We have shown that bacterially expressed recombinant ERp57/GRP58 protein contains a thiol-dependent reductase activity and that its active sites are Cys residues located in the two Trp-Cys-Gly-His-Cys-Lys motifs. On a molar basis, ERp57/GRP58 appeared to be almost half to one-third as potent as thioredoxin. A new isozyme of oxidoreductase was previously purified from rat hepatic microsomes with a partial amino acid sequence identical to that of rat ERp57/GRP58 (Srivastava et al., 1991). Though not conclusive, it is very likely that this oxidoreductase is identical to ERp57/GRP58 underlining our result that ERp57/GRP58 contains thiol-dependent reductase activity. Recently, a 60-kDa protein similar to ERp57/GRP58 was purified from the rough endoplasmic reticulum (ER) of rat liver and it exhibited thiol-group-related proteolytic activity (Urade et al., 1992). Another report showed that an extract of *E. coli* expressing ERp57/GRP58 protein contained PDI activity (Srivastava et al., 1993). Collectively, ERp57/GRP58 is thought to be a protein with multifunctional activities. It was shown very recently that either PDI or ERp72 can act as a molecular chaperone (Kuznetsov et al., 1994; Nigam et al., 1994). Considering the close similarities between ERp57/GRP58, PDI, and ERp72 with regard to the primary sequence and the functional activities, as described above, ERp57/GRP58 may also function as a molecular chaperone.

The C-terminal sequence of ERp57/GRP58 (Gln-Glu-Asp-Leu) is similar to those of PDI (Lys-Asp-Glu-Leu) and ERp72 (Lys-Glu-Glu-Leu). However, we have shown that, unlike PDI or ERp72, ERp57/GRP58 is secreted into the culture medium and that the C-terminal Gln-Glu-Asp-Leu sequence does not serve sufficiently as an ER-retention signal sequence. Supporting our results, it was discovered very recently that a murine colon carcinoma cell line, colon26, secretes a significant amount of ERp57/GRP58 into culture medium (Kozaki et al., 1994). On the other hand, Mazzarella et al. (1994) showed that ERp57/GRP58 is retained in the ER and is not secreted using the transient expression system of COS cells. Although we do not have a definite explanation for this discrepancy, it may be due to the difference in host cells or expression systems. As a soluble factor, ERp57/GRP58 might have its receptor on the target cell surface. Alternatively, a specific reductase protein may act as an ERp57/GRP58 receptor. It is likely that ERp57/GRP58 regulates the extracellular redox potential through its soluble form as well as the intracellular redox activity.

Transformation-specific alterations of cellular proteins may encompass the induced synthesis of proteins at elevated levels in transformed cells, or the transformation-specific modifications of proteins also expressed in normal cells. We have shown that, in NRK cells, the ERp57/GRP58 expression was induced by the transformation with various kinds of oncogenes. Furthermore, in NIH3T3 cells transformed with v-*src*, activated c-*src* (Y527F) and c-*src*, the expression level of ERp57/GRP58 was induced in proportion to the transforming abilities of the oncogenes. Although many kinds of proteins have been described to be induced in *ras* or *src* transformants, enhanced expression of ERp57/GRP58 in association with oncogenic transformation in mammalian cells has not been reported. Thioredoxin protein level as well is generally higher in actively growing tissues and an increase in the level of thioredoxin mRNA has been seen in v-*src*-transformed chicken embryo fibroblasts (Jones and Luk, 1988). It is possible that, for oncogenic activity to be fully exerted in physiological conditions, elevated redox activities by ERp57/GRP58 or thioredoxin are required. Alternatively, activated redox potentials may serve to maintain some features of transformed phenotypes. Human thioredoxin was originally identified as a factor derived from adult leukemia T-cells (Tagaya et al., 1989) in which thioredoxin contains interleukin-2-receptor-inducing and growth stimulatory activity behaving in an autocrine manner. Thioredoxin is thus thought to be involved in the pathogenesis of adult T-cell leukemia (Wakasugi et al., 1990). Furthermore, in peripheral blood mononuclear cells, the expression of thioredoxin mRNA is enhanced by mitogens or phorbol esters, suggesting a possible involvement of thioredoxin in the lymphocyte activation. It was previously reported that activation of Jurkat cells with mitogens or phorbol esters leads to increased expression of ERp57/GRP58 mRNA (Goldfien et al., 1991). Thus, it is quite likely that the elevated expression of ERp57/GRP58 or thioredoxin with redox potential should be a biologically significant event.

Evidence is accumulating indicating the crucial role of thiol-reducing agents for signal transduction. DNA binding of the *fos-jun* heterodimer is modulated by redox regulation of a single conserved Cys residue in the DNA-binding domains of the two proteins (Abate et al., 1990). DNA binding of *v-rel* protein is also subject to redox control through the conserved Cys residue at the Arg-Xaa-Xaa-Arg-Xaa-Arg-Xaa-Xaa-Cys motif which is conserved in all *rel*/NF-κB proteins (Kumar et al., 1992). A receptor tyrosine kinase (coded by the gene *ltk*) is regulated via changes in the cellular redox potential and its kinase activity is augmented by the formation of disulfide-linked multimers (Bauskin et al., 1991). These facts suggest that thiol/disulfide

redox potentials regulate DNA−protein and protein−protein interactions through Cys residue(s). Although regulatory factors of redox potentials *in vivo* have not yet been identified, ERp57/GRP58, PDI, and thioredoxin are interesting candidates because they can exert thiol-dependent catalytic activity through the Trp-Cys-Gly-His/Pro-Cys-Lys motif.

We thank H. Toyoshima for a human placental cDNA library and H. Okayama for NRK-derived cell lines. This work was supported in part by grants from the Ministry of Education, Science and Culture of Japan.

REFERENCES

Abate, C., Patel, L., Rauscher III, F. J. & Curran, T. (1990) Redox regulation of fos and jun DNA-binding activity *in vitro*, *Science 249*, 1157−1161.

Bauskin, A. R., Alkalay, I. & Ben-Neriah, Y. (1991) Redox regulation of a protein tyrosine kinase in the endoplasmic reticulum, *Cell 66*, 685−696.

Bennett, C. F., Balcarek, J. M., Varrichio, A. & Crooke, S. T. (1988) Molecular cloning and complete amino-acid sequence of form-I phosphoinositide-specific phospholipase C, *Nature 334*, 268−270.

Freedman, R. B. (1989) Protein disulfide isomerase: multiple roles in the modification of nascent secretory proteins, *Cell 57*, 1069−1072.

Gething, M. J. & Sambrook, J. (1992) Protein folding in the cell, *Nature 355*, 33−45.

Goldfien, R. D., Seaman, W. E., Hempel, W. M. & Imboden, J. B. (1991) Divergent regulation of phospholipase C-α and phospholipase C-γ transcripts during activation of a human T cell line, *J. Immunol. 146*, 3703−3708.

Haugejörden, S. M., Srinivasan, M. & Green, M. (1991) Analysis of the retention signals of two resident luminal endoplasmic reticulum proteins by *in vitro* mutagenesis, *J. Biol. Chem. 266*, 6015−6018.

Hempel, W. M. & DeFranco, A. L. (1991) Expression of phospholipase C isozymes by murine B lymphocytes, *J. Immunol. 146*, 3713−3720.

Hendershot, L. M. (1990) Immunoglobulin heavy chain and binding protein complexes are dissociated *in vivo* by light chain addition, *J. Cell Biol. 111*, 829−837.

Hirai, H. & Varmus, H. E. (1990) SH2 mutants of c-*src* that are host dependent for transformation are *trans*-dominant inhibitors of mouse cell transformation by activated c-*src*, *Genes & Dev. 4*, 2342−2352.

Hirano, N., Shibasaki, F., Kato, H., Sakai, R., Tanaka, T., Nishida, J., Yazaki, Y., Takenawa, T. & Hirai, H. (1994) Molecular cloning and characterization of a cDNA for bovine phospholipase C-α. Proposal of redesignation of phospholipase C-α, *Biochem. Biophys. Res. Commun. 204*, 375−382.

Holmgren, A. (1979) Thioredoxin catalyzes the reduction of insulin disulfides by dithiothreitol and dihydrolipoamide, *J. Biol. Chem. 254*, 9627−9632.

Jones, S. W. & Luk, K. C. (1988) Isolation of a chicken thioredoxin cDNA clone. Thioredoxin mRNA is differentially expressed in normal and Rous sarcoma virus-transformed chicken embryo fibroblasts, *J. Biol. Chem. 263*, 9607−9611.

Kozaki, K., Miyaishi, O., Asai, N., Iida, K., Sakata, K., Hayashi, M., Nishida, T., Matsuyama, M., Shimizu, S., Kaneda, T. & Saga, S. (1994) Tissue distribution of ERp61 and association of its increased expression with IgG production in hybridoma cells, *Exp. Cell Res. 213*, 348−358.

Kumar, S., Rabson, A. B. & Gelinas, C. (1992) The RxxRxRxxC motif conserved in all Rel/κ B proteins is essential for the DNA-binding activity and redox regulation of the v-Rel oncoprotein, *Mol. Cell. Biol. 12*, 3094−3106.

Kuznetsov, G., Chen, L. B. & Nigam, S. K. (1994) Several endoplamic reticulum stress proteins, including ERp72, interact with thyroglobulin during its maturation, *J. Biol. Chem. 269*, 22990−22995.

Lee, A. S. (1981) The accumulation of three specific proteins related to glucose-regulated proteins in a temperature-sensitive hamster mutant cell line K12, *J. Cell Physiol. 106*, 119−125.

Lee, A. S. (1987) Coordinated regulation of a set of genes by glucose and calcium ionophores in mammalian cells, *Trends. Biochem. Sci. 12*, 20−23.

Martin, J. L., Pumford, N. R., LaRosa, A. C., Martin, B. M., Gonzaga, H. M., Beaven, M. A. & Pohl, L. R. (1991) A metabolite of halothane covalently binds to an endoplasmic reticulum protein that is highly homologous to phosphatidylinositol-specific phospholipase C-α but has no activity, *Biochem. Biophys. Res. Commun. 178*, 679−685.

Mazzarella, R. A., Marcus, N., Haugejörden, S. M., Balcarek, J. M., Baldassare, J. J., Roy, B., Li, L. J., Lee, A. S. & Green, M. (1994) Erp61 is GRP58, a stress-inducible luminal endoplasmic reticulum protein, but is devoid of phosphatidylinositide specific phospholipase C activity, *Arch. Biochem. Biophys. 308*, 454−460.

Mazzarella, R. A., Srinivasan, M., Haugejörden, S. M. & Green, M. (1990) ERp72, an abundant luminal endoplasmic reticulum protein, contains three copies of the active site sequences of protein disulfide isomerase, *J. Biol. Chem. 265*, 1094−1101.

Melero, J. A. & Smith, A. E. (1978) Possible transcriptional control of three polypeptides which accumulate in a temperature-sensitive mammalian cell line, *Nature 272*, 725−727.

Melnick, J., Aviel, S. & Argon, Y. (1992) The endoplasmic reticulum stress protein GRP94, in addition to BiP, associates with unassembled immunoglobulin chains, *J. Biol. Chem. 267*, 21303−21306.

Nigam, S. K., Goldberg, A. L., Ho, S., Rohde, M. F., Bush, K. T. & Sherman, M. Y. (1994) A set of endoplasmic reticulum proteins possessing properties of molecular chaperones includes Ca^{2+}-binding proteins and members of the thioredoxin superfamily, *J. Biol. Chem. 269*, 1744−1749.

Pihlajaniemi, T., Helaakoski, T., Tasanen, K., Myllyla, R., Huhtala, M. L., Koivu, J. & Kivirikko, K. I. (1987) Molecular cloning of the β-subunit of human prolyl 4-hydroxylase. This subunit and protein disulphide isomerase are products of the same gene, *EMBO J. 6*, 643−649.

Sambrook, J., Fritsch, E. F. & Maniatis, T. (1989) *Molecular cloning: a laboratory manual*, 2nd edn, Cold Spring Harbor Laboratory, Cold Spring Harbor NY.

Srinivasan, S. R., Radhakrishnamurthy, B. & Berenson, G. S. (1975) Studies on the interaction of heparin with serum lipoproteins in the presence of Ca^{2+}, Mg^{2+}, and Mn^{2+}, *Arch. Biochem. Biophys. 170*, 334−340.

Srivastava, S. P., Chen, N. Q., Liu, Y. X. & Holtzman, J. L. (1991) Purification and characterization of a new isozyme of thiol:protein-disulfide oxidoreductase from rat hepatic microsomes. Relationship of this isozyme to cytosolic phosphatidylinositol-specific phospholipase C form 1A, *J. Biol. Chem. 266*, 20337−20344.

Srivastava, S. P., Fuchs, J. A. & Holtzman, J. L. (1993) The reported cDNA sequence for phospholipase C α encodes protein disulfide isomerase, isozyme Q-2 and not phospholipase-C, *Biochem. Biophys. Res. Commun. 193*, 971−978.

Tagaya, Y., Maeda, Y., Mitsui, A., Kondo, N., Matsui, H., Hamuro, J., Brown, N., Arai, K., Yokota, T., Wakasugi, H. & Yodoi, J. (1989) ATL-derived factor (ADF), an IL-2 receptor/Tac inducer homologous to thioredoxin; possible involvement of dithiol-reduction in the IL-2 receptor induction, *EMBO J. 8*, 757−764.

Urade, R., Nasu, M., Moriyama, T., Wada, K. & Kito, M. (1992) Protein degradation by the phosphoinositide-specific phospholipase C-α family from rat liver endoplasmic reticulum, *J. Biol. Chem. 267*, 15152−15159.

von Heijne, G. (1986) A new method for predicting signal sequence cleavage sites, *Nucleic Acids Res. 14*, 4683−4690.

Wakasugi, N., Tagaya, Y., Wakasugi, H., Mitsui, A., Maeda, M., Yodoi, J. & Tursz, T. (1990) Adult T-cell leukemia-derived factor/thioredoxin, produced by both human T-lymphotropic virus type I- and Epstein-Barr virus-transformed lymphocytes, acts as an autocrine growth factor and synergizes with interleukin 1 and interleukin 2, *Proc. Natl Acad. Sci. USA 87*, 8282−8286.

D

Structural Analysis of Alzheimer's β(1–40) Amyloid: Protofilament Assembly of Tubular Fibrils

Sergey B. Malinchik, Hideyo Inouye, Karen E. Szumowski, and Daniel A. Kirschner
Department of Biology, Boston College, Chestnut Hill, Massachusetts 02167-3811 USA

ABSTRACT Detailed structural studies of amyloid fibrils can elucidate the way in which their constituent polypeptides are folded and self-assemble, and exert their neurotoxic effects in Alzheimer's disease (AD). We have previously reported that when aqueous solutions of the N-terminal hydrophilic peptides of AD β-amyloid (Aβ) are gradually dried in a 2-Tesla magnetic field, they form highly oriented fibrils that are well suited to x-ray fiber diffraction. The longer, more physiologically relevant sequences such as Aβ(1–40) have not been amenable to such analysis, owing to their strong propensity to polymerize and aggregate before orientation is achieved. In seeking an efficient and inexpensive method for rapid screening of conditions that could lead to improved orientation of fibrils assembled from the longer peptides, we report here that the birefringence of a small drop of peptide solution can supply information related to the cooperative packing of amyloid fibers and their capacity for magnetic orientation. The samples were examined by electron microscopy (negative and positive staining) and x-ray diffraction. Negative staining showed a mixture of straight and twisted fibers. The average width of both types was ~70 Å, and the helical pitch of the latter was ~460 Å. Cross sections of plastic-embedded samples showed a ~60-Å-wide tubular structure. X-ray diffraction from these samples indicated a cross-β fiber pattern, characterized by a strong meridional reflection at 4.74 Å and a broad equatorial reflection at 8.9 Å. Modeling studies suggested that tilted arrays of β-strands constitute tubular, 30-Å-diameter protofilaments, and that three to five of these protofilaments constitute the Aβ fiber. This type of structure—a multimeric array of protofilaments organized as a tubular fibril—resembles that formed by the shorter Aβ fragments (e.g., Aβ(6–25), Aβ(11–25), Aβ(1–28)), suggesting a common structural motif in AD amyloid fibril organization.

INTRODUCTION

One of the fundamental problems in Alzheimer's disease (AD) research is to determine what drives the formation of amyloid fibrils from specific polypeptide fragments of the Aβ precursor protein. Amyloid fibrils and their accumulation as deposits in the neuropil can profoundly affect the functioning of the central nervous system, perhaps by neurotoxic mechanisms (Mattson and Rydel, 1996). To characterize the way in which the peptides assemble and exert their effects, we have been studying in vitro fibrilogenesis by using x-ray fiber diffraction and electron microscopy. We found that highly oriented fibrils for x-ray diffraction could be attained by gradually drying the peptide solution in a 2-Tesla magnetic field (Inouye et al., 1993, and references cited therein). Our previous experiments mainly utilized peptide fragments corresponding to the putative extracellular domain of Aβ, although some 40-mers were also studied, including primate, rodent, and Dutch-hemorrhagic analogs (Fraser et al., 1992). The difficulty in undertaking fiber diffraction from the longer, more physiologically relevant peptides is that, unlike most of the shorter peptides, the assembled fibers do not easily orient in a magnetic field. This results in more overlap among the x-ray reflections, making, in turn, the diffraction patterns considerably more difficult to interpret. However, because the 1–40 and 1–42 fragments are the major polypeptides found in amyloid deposits in AD, we have sought improved methods for producing from the full-length peptides oriented samples that are suitable for x-ray fiber diffraction.

The general poblem of preparing oriented fiber samples was recognized over 50 years ago in the pioneering work of Bernal and Fankuchen (1941) with tomato mosaic virus fibers. The significance of our current study arises not only because the highly ordered structure can be analyzed more easily by x-ray diffraction, but also the assembly process itself (from soluble peptide to insoluble fibers) may simulate a portion of the pathophysiological process leading to fibril formation in AD brains. Given that the fibrillar form as opposed to the soluble form may exert neurotoxicity, such as oxidant stress and activation of microglia (Mattson and Rydel, 1996), the molecular structural information of the fibrillar and soluble forms of the full sequence 1–40 may be fundamental to understanding neurodegeneration. One of the questions addressed here, therefore, pertains to that feature of the molecular organization of Aβ(1–40), which exerts the cytotoxic effects.

In the current study, a "drop test" using polarized light microscopy was newly developed to quickly test whether the peptides treated under different conditions can be oriented into well-aligned fibers. Birefringent samples were subsequently examined in the electron microscope and by x-ray diffraction. We demonstrate here that assemblies of Aβ(1–40) can become well oriented in a magnetic field after the bulk peptide solution is stored in the refrigerator for several months. Electron microscopy indicates that the

Received for publication 11 March 1997 and in final form 27 May 1997.
Address reprint requests to Dr. Daniel A. Kirschner, Department of Biology, Boston College, 140 Commonwealth Avenue, Chestnut Hill, MA 02167-3811. Tel.: 617-552-0211; Fax: 617-552-2011; E-mail: daniel.kirschner@bc.edu.

0006-3495/98/01/537/09 $2.00

peptides formed both twisted fibers of average diameter ~70 Å and pitch 460 Å, and straight fibers with the same diameter. Modeling the fibril structure from the x-ray diffraction data indicated that the fibril was tubular and was formed by a multimeric array of protofilaments.

MATERIALS AND METHODS

Aβ(1–40) peptide

We tested Aβ(1–40) peptides from three different sources: Bachem California (Torrance, CA; lot number ZM365; peptide purity >99% by HPLC); Dr. David B. Teplow (custom synthesized at Harvard Medical School; peptide purity is >99% by diphenyl reverse phase-HPLC, and ~92% by RP-HPLC) on a PLRP-5 column (Polymer Laboratories, Amherst, MA); and Quality Controlled Biochemicals (Hopkinton, MA; lot number 03013608; peptide purity >99% by HPLC; peptide provided by Dr. John E. Maggio).

Dry drop test by polarized light microscopy

Owing to the high cost of synthetic peptides and our need to survey a variety of conditions for peptide assembly and orientation, we sought to develop a method that utilizes microgram quantities of peptide for rapid screening. We found that examining the birefringence of a small drop of peptide solution could supply information related to the aggregation properties of β-amyloid fibers and their capacity for orientation in a magnetic field. Thus, 0.5-μl-aliquot drops of amyloid peptide solutions at concentrations of 5–10 mg/ml were allowed to dry on siliconized glass surfaces. The protein tends to concentrate along the circular border at the liquid-glass interface. Birefringence of the dried drop was checked by a polarizing microscope.

We tested a number of available short β-amyloid fragments and compared the results with their corresponding x-ray diffraction patterns (see Inouye et al., 1993). For all fragments tested, which included Aβ(11–28), Aβ(13–28), Aβ(11–25), Aβ(9–28), and Aβ(19–28), we found a clear correlation between the extent of birefringence in the dry drop and the quality of the peptide orientation in a magnetic field. The latter, which we term "crystallinity," was judged from the mosaic spread of the x-ray reflections and the presence of Bragg reflections on layer lines.

Electron microscopy

For thin sectioning, peptide samples were dissolved in water at 10 mg/ml and concentrated by evaporation to ~200 mg/ml. The resulting peptide gels were fixed by exposure to glutaraldehyde vapor and then to osmium tetroxide vapor. Subsequently, the gels were immersion-fixed in 2% glutaraldehyde (aq.) and 2% osmium tetroxide (aq.), stained en bloc with 4% uranyl acetate in 50% ethanol, dehydrated through a series of ethanols and propylene oxide, and embedded in Poly Bed 812. The sections were viewed in a JEOL 1200 EX electron microscope at 120 kV.

For negative staining, peptide solutions at concentrations of ~2 mg/ml were placed on carbon-coated, Formvar-covered copper grids, fixed with 0.5% glutaraldehyde and stained with 2% (wt/vol) uranyl acetate. Samples were observed in a JEOL 1200 EX electron microscope operated at 120 kV. Calibration of the micrographs was carried out with tropomyosin paracrystals (kindly provided by Dr. Carolyn Cohen, Brandeis University, Waltham, MA).

X-ray diffraction

Sample

Peptide solutions at ~5 mg/ml in distilled water were stored in the refrigerator for a few days to a few months. The samples for x-ray diffraction experiments were prepared as detailed previously (Inouye et al., 1993). Briefly, the peptide solutions were introduced into siliconized glass capillaries, which were then placed in 2-Tesla permanent magnets (Oldenbourg and Phillips, 1986) and allowed to dry under ambient temperature and humidity.

Data collection

X-ray patterns were collected using nickel-filtered and double-mirror-focused CuKα radiation from a GX-6 rotating-anode x-ray generator (Elliott-Marconi Avionics, Hertfordshire, England) with a 200-μm focal spot, and operated at 30 kV and 40 mA. A helium tunnel was placed in the x-ray path to reduce air scatter. Patterns were recorded on flat, direct-exposure x-ray film (Eastman Kodak) for 1–3 days. The specimen-to-film distance was 71.8 mm, as calibrated by the known spacings of NaCl (3.258 Å and 2.821 Å).

Densitometry and measurement of the intensity

Densitometry to quantitate the intensities was carried out as previously described (Nguyen et al., 1995). Briefly, diffraction patterns were digitized on a 100-μm raster using a VEXCEL scanner operated by the program VXSCAN. The two-dimensional intensities were displayed with SCOPE5 (Tibbitts and Caspar, 1993). The intensity curve was obtained after subtraction of the background, which was fit by polynomial or exponential equations. For precise measurement of the spacings of the reflections, the corresponding intensity peaks were fit by a Gaussian function with the program PeakFit (Jandel Scientific Software).

Model calculations

The equatorial diffraction patterns were calculated according to $I(R) = F^2(R)Z(R)/NR$. Here N is the number of subunits, $F(R) = 2\pi[r_i J_0(2\pi r_1 R) + r_2 J_0(2\pi r_2 R)]$, where r_1 and r_2 are the outer and inner radii of a thin-walled cylinder, and $Z(R) = \Sigma_j \Sigma_k J_0(2\pi r_{jk} R)$, where $r_{jk} = |r_j - r_k|$ for the distance between the subunit vectors in cylindrical coordinates (Vainshtein, 1966). The denominator R corrects for the mosaic spread of the intensity, because the observed intensity was derived from a strip scan along the equator.

RESULTS

Conditions for sample preparation

The drop test for the Aβ(1–40) peptides was carried out systematically to seek promising conditions for fiber growth and orientation. As a positive control, we used peptide Aβ(11–25), which, when fibrillar, orients readily in a magnetic field and gives sharp x-ray diffraction (Inouye et al., 1993), and gives very strong birefringence in the drop test. When lyophilized peptides from the three different sources of Aβ(1–40) (see Materials and Methods) were dissolved in distilled water and incubated at 24°C for 3–5 days, all showed very poor birefringence in the drop test (Fig. 1, *a* and *b*), and the concentrated samples prepared from these peptide solutions did not show any response to a 2-T magnetic field, as judged by the lack of orientation of birefringent domains during the drying period. X-ray diffraction patterns from the partially dried pellets showed very poor orientation, with only weak reflections suggestive of a cross-β structure. Variations in the initial conditions—including peptide concentrations (from 0.1 to 10 mg/ml), pH (range, pH 5–9) (Fraser et al., 1991b), ionic strength, and

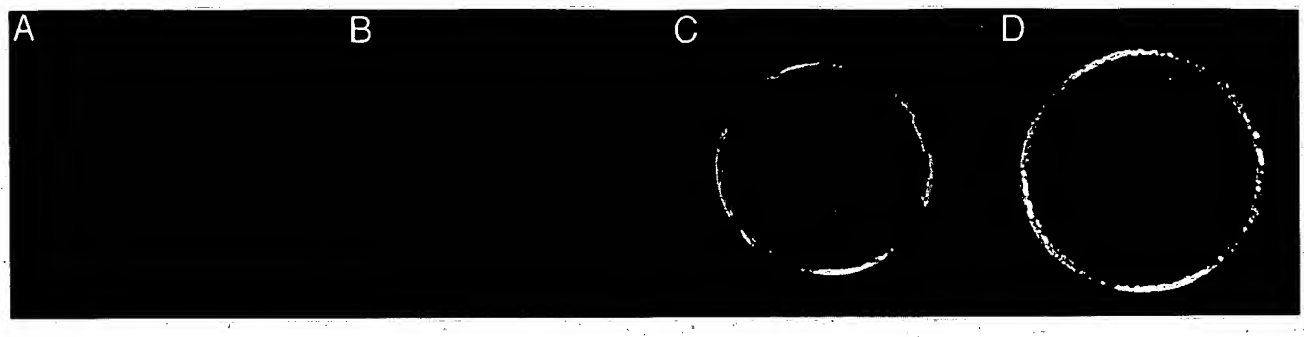

FIGURE 1 Results of the drop test. Images of dried drops of peptide solutions, viewed between crossed polarizers, suggest whether liquid crystalline domains have formed in the peptide solutions. (*A* and *B*) Aβ(1–40) peptide solutions (5 mg/ml) from different peptide sources (Bachem (*A*) and QCB (*B*)) up to 30 days after dissolving in distilled water. Birefringence is absent or very weak. (*C*) Aβ(1–40) peptide (QCB) after 3 months' storage in the cold shows strong birefringence. (*D*) Aβ(11–25) peptide a few hours after dissolving in water indicates strong birefringence. While drying under ambient conditions, the peptide solutions of *C* and *D* showed birefringent domains that could be oriented in a 2-T magnetic field.

presence of sulfate ions (Fraser et al., 1992)—did not improve the ability of the fibers to orient in the magnetic field. Indeed, electron microscopy invariably showed the formation of unbranched, typical-looking fibers with considerable variation in length.

The idea of exploring the time factor in fiber formation was based on the finding that aqueous solutions of peptide Aβ(1–40) synthesized by Quality Controlled Biochemicals (QCB, Hopkinton, MA) are higly monomeric and stable (Dr. John E. Maggio, personal communication). Because previous reports have shown that storage of Aβ peptides at low concentration leads gradually to changes in their secondary structure and aggregation properties (Barrow and Zagorski, 1991; Barrow et al., 1992; Pike et al., 1991a,b), we thought it worthwhile to monitor fiber formation and magnetic orientation in peptide preparations that were known to be relatively stable.

After the QCB peptide solution was kept at an initial concentration of 5 mg/ml in the refrigerator for three months, the drop test revealed a strong birefringence comparable to that shown for Aβ(11–25). Fig. 1, *b* and *c*, illustrates the drop tests for Aβ(1–40) at 10 days and at 3 months after lyophilized peptide is dissolved in water. Drop tests after 1 and 2 months did not show any difference from that at 10 days. By contrast, the drop test for Aβ(11–25) 1 h after the peptide was dissolved in water showed prominent birefringence (Fig. 1 *d*).

Samples used for electron microscopy and x-ray diffraction were preparations of Aβ(1–40) from QCB that had been stored for 3 months in the refrigerator. During drying in the capillary tube, the peptide solution showed birefringent domains that could be oriented in the 2-T magnetic field. The resulting thin pellet could be rotated to show uniform extinction when viewed face on, and was used for fiber diffraction (see Fig. 2).

Fiber structure of Aβ(1–40) observed by electron microscopy

Negative staining of QCB Aβ(1–40) samples showed long, unbranched fibers. There was considerable variation in the appearance of the fiber structure, even on the same grids. Generally, the fibrillar assemblies could be divided into two main populations: one consisting of narrow, straight fibers, and the other consisting of twisted, paired fibers (Fig. 3, *a*

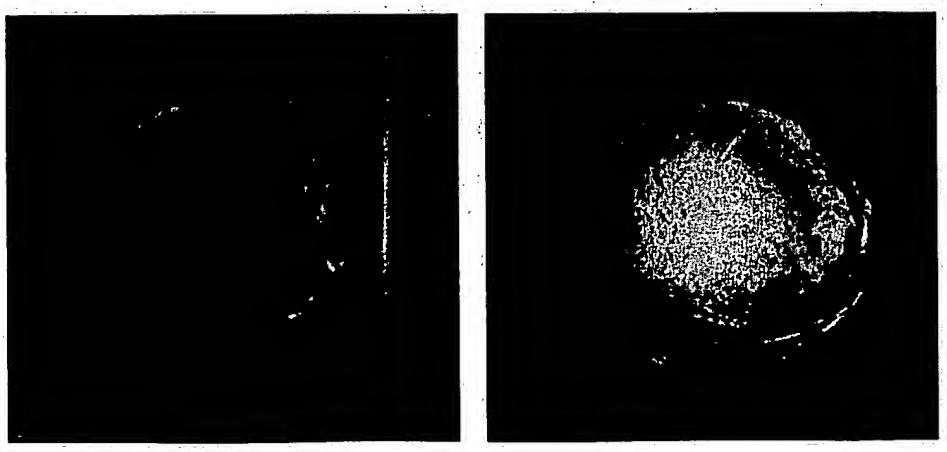

FIGURE 2 The final pellets formed by peptide solutions *C* and *D* of Fig. 1. (*left*) Aβ(1–40); (*right*) Aβ(11–25). Viewed through a polarizing microscope, the samples show uniform extinction.

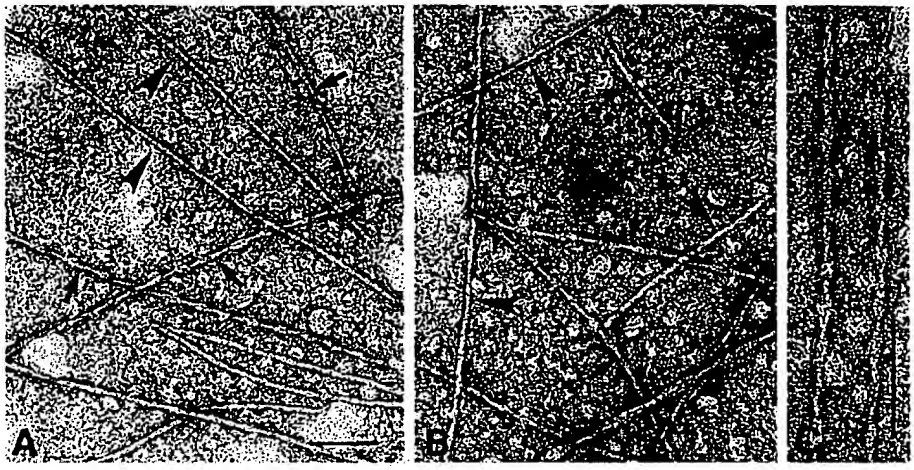

FIGURE 3 Electron micrographs of negative-stained preparations. (*A* and *B*) "Aged" Aβ(1–40) samples (QCB peptide) exhibited a multitude of long fibers, falling primarily into one of two types: regularly twisted fibers (*arrows*) and straight, relatively smooth fibers (*arrowheads*). Scale bar, 1000 Å. (*C*) Higher magnification of two twisted fibers from an "aged" sample of QCB Aβ(1–40). Scale bar, 1000 Å.

and *b*). The average fiber size for both types of structures was ~70 Å (range, 60–80 Å for smooth fibers and 50–90 Å for twisted fibers). The helical pitch of the twisted fibers was ~460 Å (range, 360–560 Å). Cross-sectioned samples of another sample (Aβ(1–40) sythesized in the laboratory of Dr. David Teplow (Harvard Medical School) (Fig. 4) showed a tubular structure, ~60 Å in diameter, with an electron-lucent center. Although there were discrete deposits of staining along the circular wall of the fiber, indicating possible subunit structures, the number of subunits constituting the tubular wall was not unambiguous from the electron micrographs.

X-ray results and interpretation

The highly birefringent Aβ(1–40) sample gave a cross-β diffraction pattern (Fig. 5) in which a sharp 4.7-Å reflection was on the meridian, and a broad 8.9-Å reflection was on the equator. In most cross-β patterns from β-amyloid analogs, an off-meridional 3.8-Å reflection is observed, but here the intensity maximum for this reflection was on the meridian. We also observed in the low-angle region a very strong and sharp equatorial reflection at 49.2 Å and two broad reflections at 19.0 Å and 13.7 Å.

Meridional diffraction

Different β-amyloid analogs appear to have in common an orthogonal unit cell with characteristic dimensions of $a \approx 9.4$ Å, $b \approx 6.6$ Å, and $c \approx 10$ Å (Inouye et al., 1993), where the *a* axis is parallel to the hydrogen bonding direction, *b* is along the chain direction, and *c* is along the intersheet direction. For the Aβ(1–40) considered here, the observed reflections on the meridian at 4.72 Å and 3.84 Å, and on the equator at 8.9 Å, were indexed as (200), (210), and (001) of the orthogonal unit cell, with $a = 9.44$ Å, $b = 6.60$ Å, and $c = 8.9$ Å.

When the fiber is aligned with the *a* axis parallel to the fiber direction, as in a classical cross-β pattern (Geddes et al., 1968), the (200) is strictly meridional, whereas the (210) is off-meridional, and the β-chains are perpendicular to the fiber axis. For the case of Aβ(1–40) previously described (Fraser et al., 1992), the (200) and the (210) were clearly off-meridional and on the meridian, respectively, indicating that the β-chains are tilted by 35.6° (*acos*(3.84/4.72)) from their perpendicular orientation. In the pattern for Aβ(1–40) described here, both the (200) and the (210) reflections appear to be on the meridian. This may be explained by rotation around the fiber axis (cylindrical averaging), which enhances the relative intensity of the meridional reflections relative to the off-meridional ones, and by translational and angular disorders within the fibers, which broaden the off-meridional reflections on the layer lines but not on the meridian and equator (Inouye, 1994).

Equatorial diffraction

The equatorial scattering and reflections arise from the axial projection of the electron density distribution. The primary peak at 49.2 Å was very sharp and strong, whereas the subsequent peaks at 19.0, 13.7 and 8.9 Å were weak and broad. The first peak can be regarded as arising from interference between objects arranged laterally on a short-range, two-dimensional lattice. If the 49.2 Å reflection is the first peak from a two-dimensional hexagonal lattice (d_{10}), the cell dimension $a = 56.8$ Å (according to $a = 2d_{10}/\sqrt{3}$, where $d_{10} = 49.2$ Å). In the case where this reflection arises from cylindrically averaged interference between only a pair of objects separated by distance *a*, the intensity maximum occurs at the primary peak of J_0, where $2\pi aR = 7.037$; therefore, $a = 55.1$ Å. Thus the separation of the objects is within the range 55–57 Å. This is slightly smaller than the 60–70-Å fiber size observed by electron microscopy of negatively and positively stained samples.

Compared to the prominent arc at 49 Å, the three reflections at 19.0-, 13.7-, and 8.9-Å spacings were diffuse and had more uniform, circular intensity distributions. The reciprocal separation between 13.7 Å and 8.9 Å was used to estimate that the separation between two cylindrically averaged pair of objects was ~28 Å. It appears, therefore, that

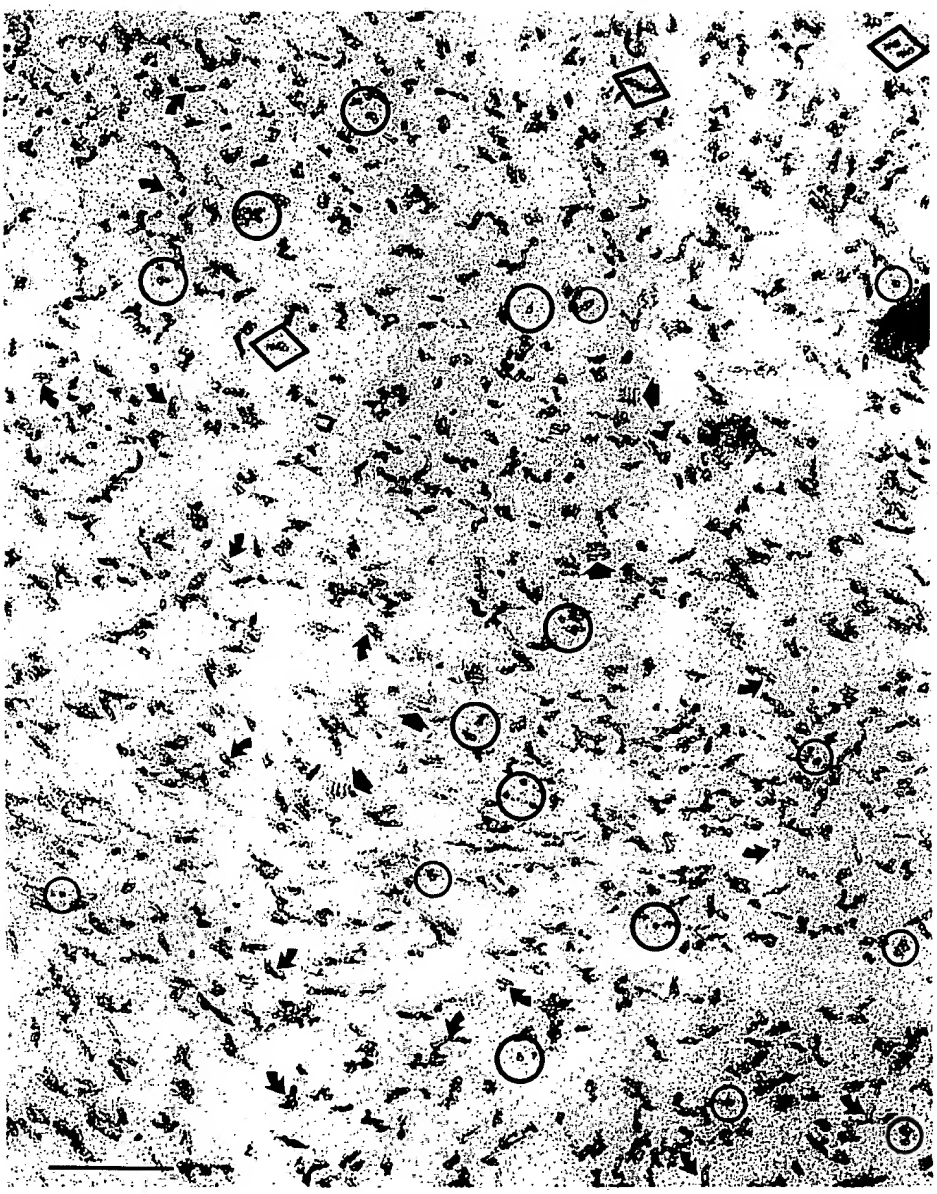

FIGURE 4 Electron micrograph of thin-sectioned preparation. A sample of Aβ(1–40) (synthesized by Dr. D. B. Teplow, Harvard Medical School), after 1 week of storage, displayed a tubular structure (~60 Å in diameter) with an electron-lucent center. Note the circular profiles where the fibers have been cut in cross section (*open circles*), the straw like outlines where the fibers were cut longitudinally (*curved arrows*), parallel alignment of closely apposed fibers (*straight arrows*), and cross-sectional views of such arrays (*open diamonds*). Scale bar, 1000 Å.

the three broad equatorial reflections at wide angle may arise from sampling of a very broad intensity maximum centered in this region.

Based on these considerations, we suggest the following model: pairs of β-sheets, with an intersheet distance of ~9 Å, build up a tubular cylinder (or protofilament; see below). The β-sheets are centered at radii $r_1 \approx 14$ Å (28 Å/2) and $r_2 \approx 5$ Å, respectively. This model is similar to the one proposed in our low-resolution studies of the shorter peptide Aβ(1–28) (Kirschner et al., 1987), and in recent x-ray analysis of transthyretin (TTR) amyloid (Blake and Serpell, 1996). When calculated with $r_1 = 14.3$ Å and $r_2 = 5.3$ Å, this model gives three broad equatorial reflections at spacings of 22, 13, and 8.9 Å, as shown in Fig. 6. The spacings of these reflections are determined mostly by the outer radius of the cylinder and are much less sensitive to the inner radius. The apparent intersheet reflection at 8.9 Å on the film does not correspond directly to the actual intersheet distance because of the cylindrical symmetry.

A single 28-Å-wide tubular cylinder, as described above, does not by itself account for the strong low-angle reflection at 49.2 Å. This intensity maximum derives, rather, from cylindrically averaged interference between objects that are separated by a distance of ~55 Å. Because negative staining shows that the fiber width is ~70 Å, the 28-Å-wide tubular structure would be a protofilament of the fiber. The arrangement of protofilaments along a circle with radius $r_o = 55$ Å/2 would account for both the small-angle and wide-angle reflections. From the geometrical constraint of $r_s = r_o \sin(\pi/N)$, where r_s(= 14.3 Å) and r_o(= 55 Å/2) are radii of the protofilament and fiber, respectively, the maximum number N of protofilaments is 5.7.

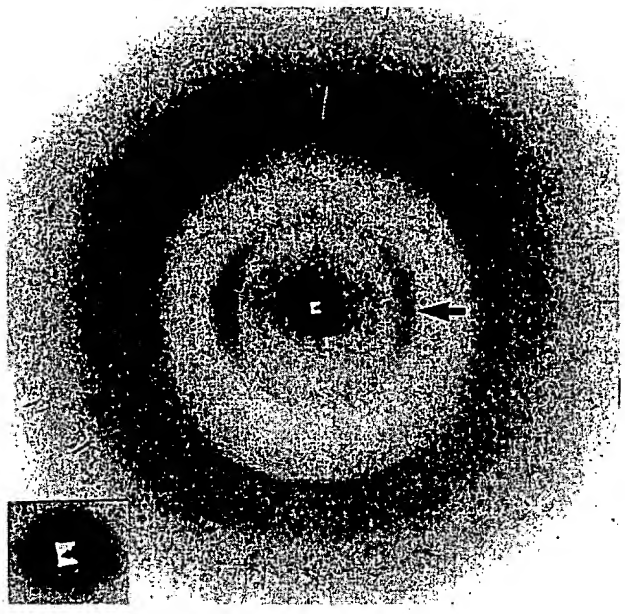

FIGURE 5 X-ray diffraction pattern from Aβ(1–40). The exposure time was 113 h, and the specimen-to-film distance was 71.8 mm. The spacings of the predominant reflections observed on the equator (E) and meridian (M) are 49.2 Å (E), 19.0 Å (E), 13.7 Å (E), 8.9 Å (E, *arrow*), 4.7 Å (M, *arrowhead*), and 3.8 Å (M). The inset shows, at higher magnification, the sharply arced reflection at 49.2 Å spacing.

The calculated intensity for a fibril consisting of 3, 4, and 5 protofilaments arranged on a circle of radius r_o is shown in Fig. 6. Radii of 23.5 Å for three protofilaments and 26 Å for four or five protofilaments were found by fitting the first interference peak to the observed position at 49.2 Å spacing. A fibril model consisting of only two protofilaments did not give any peak in this region, and a model consisting of six protofilaments was not plausible, because of steric considerations. These calculations show that the reflection at 49.2 Å may arise from protofilament interference, but the calculated intensity is stronger than the observed one. A disorder effect, not yet identified, may result in a smaller observed intensity of the 49.2 Å reflection, and may also reduce the influence of interference on the reflections at 22-, 13-, and 9-Å spacings. The intensity maxima at ~50 Å could also arise from interfibril interference as fibrils become closely packed in samples that are very concentrated.

Although the parameters are not optimized against the observed intensity, a likely model for the Aβ(1–40) assembly is that the 70-Å tubular fiber (average diameter) is made up of three, four, or five protofilaments and the individual protofilament is a ~30-Å-wide tubular structure whose wall is composed of a tilted array of β-chains. Although this symmetrical cross-sectional model is not ideally consistent with the twisted fiber, the cross section of which would be asymmetrical, the equatorial x-ray analysis provides an approximate model for both straight and twisted fibers.

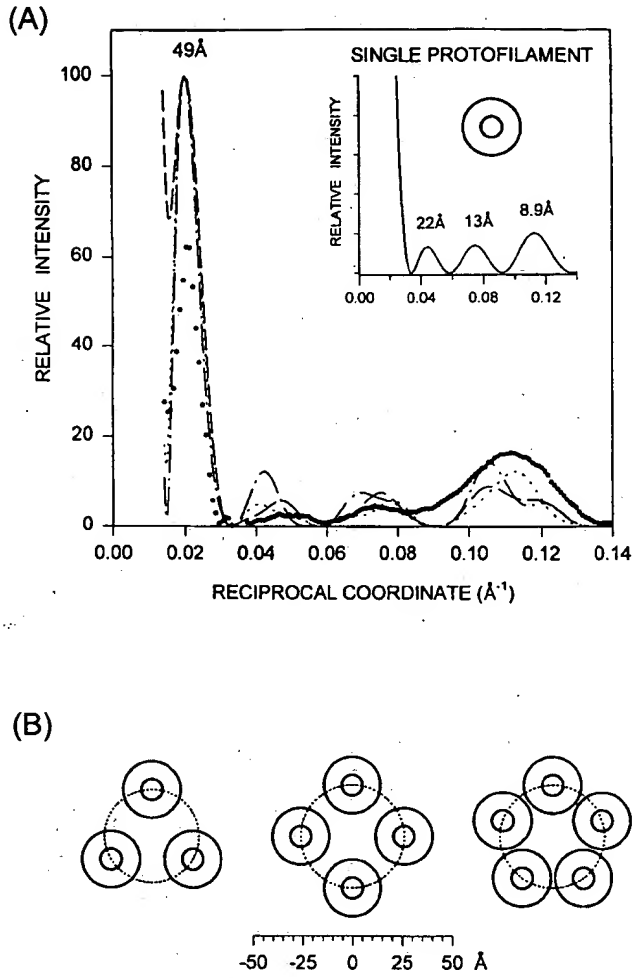

FIGURE 6 Modeling of the equatorial x-ray diffraction data from Aβ(1–40). (*A*) Experimental and calculated equatorial intensities for single (*A*, *inset*) and multiple (*B*) tubular protofilaments. For the latter, the protofilaments were arranged on the circumference of a circle whose radius was consistent with the first interference peak at 49.2 Å (see text for details). To reveal the low-angle region at ~0.02 Å^{-1}, densitometer traces of the first and second films were scaled and combined. The background was subtracted as described in Materials and Methods. Points (●), Experimental data; — —, three protofilaments; – – –, four protofilaments; — - —, five protofilaments.

DISCUSSION

Relating birefringence in drop test to magnetic orientation of fibrils

Anisotropically shaped macromolecular assemblies can be induced to orient by a strong magnetic field. The origin of the physical torque in proteins or polypeptide assemblies is diamagnetism of oriented aromatic groups (Pauling, 1936) and of oriented planar peptide bonds (Worcester, 1978; Pauling, 1979). In general, protein structures with substantial amounts of parallel α-helices will orient with the helices parallel to the magnetic field, whereas in β-pleated sheets the orientation of aromatic side chains plays a major role in the orientation of the structure as a whole.

The diamagnetic susceptibility that can be calculated from the x-ray diffraction patterns of different, oriented macromolecular assemblies is much larger than would be expected for a single assembly, suggesting that the group of assemblies orients cooperatively (Makowski, 1988). Thus, as pointed out in this paper, although an individual assembly may exhibit little or no orientation in a magnetic field, liquid crystalline domains consisting of several thousand particles are likely to orient.

These considerations can be used to explain the correlation between the drop test results and the magnetic orientation of the Aβ assemblies. During the drying of a drop of the peptide solution, the surface tension causes protein to concentrate in the circular perimeter of the drop (Fig. 1, *a* and *b*). Surface tension tends to align individual fibrils, whereas thermal effects tend to disorient them. In the case of cooperative domains consisting of parallel fibrils, the surface tension dominates the thermal effects, and so the domains show a net orientation along the periphery of the drop. Thus the birefringence in the drop test and the magnetic orientation of the preparations both likely depend on the formation of liquid crystalline domains. Long-term storage of the peptide solution in the cold ("aging") may promote formation of such domains by slowing the fibril growth and generating more uniform lengths of fibrils. In the case of Aβ(11–25), domains of parallel fibrils form within hours, whereas with Aβ(1–40), the process may require weeks or months.

Tilted β-chains

The β-structure in the current study of Aβ(1–40) showed a tilted array of orthogonal β-crystalline units in which the fiber grows in the (210) direction as opposed to the (200) (or strictly H-bonding) direction. Such tilted β-chains, having different extents of tilt angle, have been reported for different proteins. Previously, an immunoglobulin array in a single crystal showed formation of an infinite β-sheet arrangement where the β-chains were tilted from the direction normal to the long axis of the β-sheet (Schiffer et al., 1985). Studies of adenovirus fiber (Stouten et al., 1992) and transthyretin (TTR) (Hamilton et al., 1996) also show similar tilted chains. A recently reported twisted β-structure for TTR amyloid fibers (Blake and Serpell, 1996) describes a pair of polyalanine-like β-chains separated by ~10 Å in a helical array with a 115-Å pitch, with the β-chains running normal to the fiber direction.

Amphipathic nature of the sequence may produce twisted fiber

The sequence of peptide Aβ(1–40) is shown in Fig. 7. The pattern of different physical-chemical attributes (e.g., hydrophobicity, polarity, charge, side-chain size) in the Aβ(1–40) sequence was analyzed by methods involving Fourier transform and averaging (Inouye and Kirschner, 1991). The secondary structures (α-helix, α; β-structure, β; coil, c, and turn, t) were predicted according to Chou-Fasman (CH) (1978) and Garnier's (G) method with a zero decision constant (Garnier et al., 1978). The atomic coordinates (deposited in the Brookhaven Protein Data Bank, ID 1AML) were determined by solution NMR (Sticht et al., 1995). The authors (Sticht et al., 1995) (S) assigned two helices from the atomic coordinates in the sequences at Gln^{15}-Asp^{23} and Ile^{31}-Met^{35}. The first helix was predicted by the methods of Chou-Fasman and Garnier, whereas the second helix was not predicted by any method.

	Asp	Ala	Glu	Phe	Arg	His	Asp	Ser	Gly	Tyr	Glu	Val	His	His	Gln
	1	2	3	4	5	6	7	8	9	10	11	12	13	14	15
CF	α	α	α	α	-	t	t	-	β	β	α	β	α	α	β
G	α	α	α	α	α	c	c	t	t	t	t	c	c	α	α
S														α	α

	Lys	Leu	Val	Phe	Phe	Ala	Glu	Asp	Val	Gly	Ser	Asn	Lys	Gly	Ala
	16	17	18	19	20	21	22	23	24	25	26	27	28	29	30
CF	β	β	β	α	α	α	-	t	-	t	t	t	α	β	β
G	α	α	α	α	α	α	α	α	c	c	c	c	c	c	c
S	α	α	α	α	α	α	α	α							

	Ile	Ile	Gly	Leu	Met	Val	Gly	Gly	Val	Val
	31	32	33	34	35	36	37	38	39	40
CF	β	β	β	β	β	β	β	-	-	-
G	β	β	β	β	β	β	β	β	β	β
S	α	α	α	α	α					

FIGURE 7 The sequence of peptide Aβ(1–40) (See text for details).

A number of fibrillar assemblies formed by Alzheimer's Aβ analogs have been analyzed by x-ray diffraction (see Inouye et al., 1993), including the N-terminal hydrophilic and C-terminal hydrophobic domains. In addition to the twisted fibers observed for Aβ(1–40) (reported here), similar morphology has previously been found for the shorter peptide analogs near the hydrophobic C-terminus, i.e., Aβ(34–42) (Halverson et al., 1990), Aβ(22–35) (Fraser et al., 1991a), and Aβ(25–35) (Fraser et al., 1993). Aβ(22–35) shows twisted fibers with 50–60 Å for the minimum width, 120 Å for the maximum width, and 1100 Å for the pitch, which is most similar to the one observed here for Aβ(1–40). Aβ(34–42) assembles into fibers having a much larger width (85–95 Å) in the narrowest region, and Aβ(25–35) assembles into a larger sheet (150–500 Å wide). The subunit of this sheet appears to be a 30-Å-wide protofilament (Fraser et al., 1993) similar to the one discovered here for Aβ(1–40). From the correlation between fiber morphology and the primary sequence, it is likely that the twisted fiber in Aβ(1–40) may be related to the amphipathic nature of the residues at positions 22–35.

Because the x-ray diffraction patterns from the Aβ(22–35) and Aβ(25–35) assemblies (Fraser et al., 1991a, 1993) show powderlike concentric rings and do not allow definition of the fiber direction in terms of an orthogonal unit cell

of the β-sheet, it is not clear whether the amphipathic property of these peptides can be related to the tilting of the β-chain as observed in Aβ(1–40). Transformation from a twisted fiber to a straight fiber has been reported for Aβ(34–42) when it is treated by a denaturing agent (Halverson et al., 1990) and for Aβ(1–40) at high pH (Fraser et al., 1992). These data suggest that residues that are exposed to the medium have a crucial influence on the twisted fiber assembly.

A tubular ultrastructure has previously been seen in electron micrographs of cross-sectioned fibrils and has been determined by analysis of x-ray diffraction patterns from assemblies formed by the shorter, N-terminal hydrophilic Aβ peptides—e.g., Aβ(6–25), Aβ(11–28), and Aβ(1–28) (Kirschner et al., 1987; Fraser et al., 1991a,b; Inouye et al., 1993). Our finding that a multimeric array of protofilaments also constitutes the tubular fibril assembled from the longer, more physiological Aβ(1–40) suggests that this is a common structural motif in amyloid fibril organization.

Fiber structure and neurotoxicity

Both Aβ(1–40) and Aβ(25–35), which contain the sequence of Aβ(22–35), are neurotoxic in fiber form (Yan et al., 1996; El-Khoury et al., 1996), suggesting that the twisted form of the fiber or ribbon structure may harbor a molecular structure with a high affinity for the putative receptor. As indicated in the secondary structure prediction and NMR result (see above), the hydrophilic part is largely turn or coil, and the hydrophobic part is predicted to be in an extended β-chain (or was determined to be α-helical in solution). It is thus likely that the hydrophilic turn at position 22–35 (Gly^{25}-Ser^{26}-Asn^{27}-Lys^{28}) might be exposed on the surface of the Aβ(1–40) fiber and that this is the part that binds to the receptor site.

Within the same batch of peptide and even on the same EM grid two different fibers were observed, one twisted and the other straight. This is similar to the case for another hallmark structure in Alzheimer's disease, i.e., paired helical filament (PHF) (Crowther, 1991). The three-dimensional reconstruction of a PHF fiber from electron micrographs indicates that the two different forms arise from different assemblies of the subunits (Crowther, 1991). This may also be the case for the ~70-Å-wide, tubular Aβ(1–40) fiber, which is likely composed of 30-Å protofilaments, as indicated here. The diffraction from A(β1–40) shows an atypical tilt of the β-chains, which may underlie the macroscopic twist of the fibers (Chothia and Murzin, 1993). Because the fiber form of Aβ(1–40) as opposed to the soluble form is neurotoxic, the structure of the Aβ(1–40) fiber is significant neuropathologically. How different fiber assemblies can affect neurotoxicity via receptor affinity is an important question. Refined x-ray diffraction and electron microscopic image analyses with parallel studies of Aβ cytotoxicity will address this question.

We thank Dr. John E. Maggio for his generosity in providing us with the highly purified Aβ(1–40) peptide from QCB, and Dr. Walter Phillips for giving us access to the x-ray equipment in his laboratory at the Rosenstiel Center, Brandeis University (Waltham, MA).

The research was supported by an Alzheimer's Association Zenith Award to DAK, and by a research grant from the National Aeronautics and Space Administration (NAG8-1145).

REFERENCES

Barrow, C. J., A. Yasuda, P. T. Kenny, and M. G. Zagorski. 1992. Solution conformations and aggregational properties of synthetic amyloid beta-peptides of Alzheimer's disease. Analysis of circular dichroism spectra. *J. Mol. Biol.* 225:1075–1093.

Barrow, C. J., and M. G. Zagorski. 1991. Solution structures of beta peptide and its constituent fragments: relation to amyloid deposition. *Science.* 253:179–182.

Bernal, J. D., and I. Fankuchen. 1941. X-ray and crystallographic studies of plant virus preparations. *J. Gen. Physiol.* 25:111–165.

Blake, C., and L. Serpell. 1996. Synchrotron x-ray studies suggest that the core of the transthyretin amyloid fibril is a continuous β-sheet helix. *Structure.* 4:989–998.

Chothia, C., and A. G. Murzin. 1993. New folds for all-beta proteins. *Structure.* 1:217–222.

Chou, P. Y., and G. D. Fasman. 1978. Empirical predictions of protein conformation. *Annu. Rev. Biochem.* 47:251–276.

Crowther, R. A. 1991. Straight and paired helical filaments in Alzheimer disease have a common structural unit. *Proc. Natl. Acad. Sci. USA.* 88:2288–2292.

El-Khoury, J., S. E. Hickman, C. A. Thomas, L. Cao, S. C. Silverstein, and J. D. Loike. 1996. Scavenger receptor-mediated adhesion of microglia to β-amyloid fibrils. *Nature.* 382:716–719.

Fraser, P. E., L. K. Duffy, M. B. O'Malley, J. Nguyen, H. Inouye, and D. A. Kirschner. 1991a. Morphology and antibody recognition of synthetic β-amyloid peptides. *J. Neurosci. Res.* 28:474–485.

Fraser, P. E., D. R. McLachlan, J. T. Nguyen, C. A. Mizzen, and D. A. Kirschner. 1993. Structural modeling of Alzheimer Aβ peptide 25–35: comparison to α1-antitrypsin and implications for amyloid toxicity. *Neurodegeneration.* 2:155–163.

Fraser, P. E., J. T. Nguyen, H. Inouye, W. K. Surewicz, D. J. Selkoe, M. B. Podlisny, and D. A. Kirschner. 1992. Fibril formation by primate, rodent, and Dutch-Hemorrhagic analogues of Alzheimer amyloid β-protein. *Biochemistry.* 31:10716–10723.

Fraser, P. E., J. Nguyen, W. Surewicz, and D. A. Kirschner. 1991b. pH-dependent structural transitions of Alzheimer amyloid peptides. *Biophys. J.* 60:1190–1201.

Garnier, J., D. J. Osguthorpe, and B. Robson. 1978. Analysis of the accuracy and implications of simple methods for predicting the secondary structure of globular proteins. *J. Mol. Biol.* 120:97–120.

Geddes, A. J., K. D. Parker, E. D. T. Atkins, and E. Beighton. 1968. "Cross-beta" conformation in proteins. *J. Mol. Biol.* 32:343–358.

Halverson, K., P. E. Fraser, D. A. Kirschner, and P. T. Lansbury. 1990. Molecular determinants of amyloid deposition in Alzheimer's disease: conformational studies of synthetic β-protein fragments. *Biochemistry.* 29:2639–2644.

Hamilton, J. A., L. K. Steinrauf, B. C. Braden, J. R. Murrell, and M. D. Benson. 1996. Structural changes in transthyretin produced by the Ile 84 Ser mutation which result in decreased affinity for retinol-binding protein. Amyloid. *Int. J. Exp. Clin. Invest.* 3:1–12.

Inouye, H. 1994. X-ray scattering from a discrete helix with cumulative angular and translational disorders. *Acta Crystallogr.* A50:644–646.

Inouye, H., P. E. Fraser, and D. A. Kirschner. 1993. Structure of β-crystallite assemblies formed by Alzheimer β-amyloid protein analogues: analysis by x-ray diffraction. *Biophys. J.* 64:502–519.

Inouye, H., and D. A. Kirschner. 1991. Folding and function of the myelin proteins. *J. Neurosci. Res.* 28:1–17.

Kirschner, D. A., H. Inouye, L. K. Duffy, A. Sinclair, M. Lind, and D. J. Selkoe. 1987. Synthetic peptide homologous to β protein from Alzheimer disease forms amyloid-like fibrils in vitro. *Proc. Natl. Acad. Sci. USA.* 84:6953–6957.

Makowski, L. 1988. Preparation of magnetically oriented speciments for diffraction experiments. *In* Brookhaven Symposium—Synchrotron Radiation in Biology. R. M. Sweet and A. D. Woodhead, editors. New York, Plenum Press. 341–347.

Mattson, M. P., and R. Rydel. 1996. Amyloid ox-tox transducers. *Nature.* 382:674–675.

Nguyen, J. T., H. Inouye, M. A. Baldwin, R. J. Fletterick, F. E. Cohen, S. B. Prusiner, and D. A. Kirschner. 1995. X-ray diffraction of scrapie prion rods and PrP peptides. *J. Mol. Biol.* 252:412–422.

Oldenbourg, R., and W. C. Phillips. 1986. Small permanent magnet for fields up to 2.6T. *Rev. Sci. Instrum.* 57:2362–2365.

Pauling, L. 1936. The diamagnetic anisotropy of aromatic molecules. *J. Chem. Phys.* 4:673–677.

Pauling, L. 1979. Diamagnetic anisotropy of the peptide group. *Proc. Natl. Acad. Sci. USA.* 76:2293–2296.

Pike, C. J., A. J. Walencewicz, C. G. Glabe, and C. W. Cotman. 1991a. In vitro aging of beta-amyloid protein causes peptide aggregation and neurotoxicity. *Brain Res.* 563:311–314.

Pike, C. J., A. J. Walencewicz, C. G. Glabe, and C. W. Cotman. 1991b. Aggregation-related toxicity of synthetic beta-amyloid protein in hippocampal cultures. *Eur. J. Pharmacol.* 207:367–368.

Schiffer, M., C.-H. Chang, and F. J. Stevens. 1985. Formation of an infinite β-sheet arrangement dominates the crystallization behavior of lambda-type antibody light chains. *J. Mol. Biol.* 186:475–478.

Sticht, H., P. Bayer, D. Willbold, S. Dames, C. Hilbich, K. Beyreuther, R. W. Frank, and P. Esch. 1995. Structure of amyloid Aβ-(1–40)-peptide of Alzheimer's disease. *Eur. J. Biochem.* 233:293–298.

Stouten, P. F., C. Sander, R. W. H. Ruigrok, and S. Cusack. 1992. New triple-helical model for the shaft of the adenovirus fibre. *J. Mol. Biol.* 226:1073–1084.

Tibbitts, T. T., and D. L. D. Caspar. 1993. Deconvolution of disoriented fiber diffraction data using iterative convolution and local regression. *Acta Crystallogr.* A49:532–545.

Vainshtein, B. K. 1966. Diffraction of X-Rays by Chain Molecules. Elsevier Publishing Company, Amsterdam.

Worcester, D. 1978. Structural origins of diamagnetic anisotropy in proteins. *Proc. Natl. Acad. Sci. USA.* 75:5475–5477.

Yan, S. D., X. Chen, J. Fu, M. Chen, H. Zhu, A. Roher, T. Slattery, L. Zhao, M. Nagashima, J. Morser, A. Migheli, P. Nawroth, D. Stern, and A. M. Schmidt. 1996. Receptors for Alzheimer's RAGE and amyloid-β peptide neurotoxicity in Alzheimer's disease. *Nature.* 382:685–691.

G

Communication

THE JOURNAL OF BIOLOGICAL CHEMISTRY
Vol. 268, No. 5, Issue of February 15, pp. 3021-3024, 1993

β-Amyloid Peptide and a 3-kDa Fragment Are Derived by Distinct Cellular Mechanisms*

(Received for publication, September 28, 1992, and in revised form, December 7, 1992)

Christian Haass, Albert Y. Hung, Michael G. Schlossmacher‡, David B. Teplow, and Dennis J. Selkoe

From the Department of Neurology and Program in Neuroscience, Harvard Medical School, and Center for Neurologic Diseases, Brigham and Women's Hospital, Boston, Massachusetts 02115

We have analyzed the cellular processing pathways which produce the 4-kDa amyloid β-peptide (Aβ) and a 3-kDa derivative (p3) of the β-amyloid precursor protein (βAPP) found in conditioned media of tissue culture cells and in cerebrospinal fluid. Pulse-chase experiments reveal that both peptides are secreted in parallel with soluble βAPP (APP_s); no precursor-product relation between Aβ and p3 was found. The protease inhibitor leupeptin did not influence the production of either peptide. In contrast, the weak base ammonium chloride (NH_4Cl) showed a dose-dependent inhibition of Aβ production with less decrease in p3. A similar effect was observed using the monovalent ionophore monensin. Brefeldin A completely inhibited the generation of both peptides, indicating that proteases located in the endoplasmic reticulum or early Golgi are not sufficient for the production of the small peptides. Deletion of the βAPP cytoplasmic domain, which removes a consensus sequence that probably mediates reinternalization, caused an increase in secretion of both APP_s and p3 and did not abolish Aβ production. These observations suggest that completely mature βAPP within the late Golgi and/or at the cell surface is a prerequisite for Aβ production but processing within the lysosome might not be directly required. p3 appears to derive from the 10-kDa C-terminal stub of βAPP following secretion of APP_s.

Alzheimer's disease is characterized by the formation in the brain of insoluble amyloid plaques and vascular deposits consisting of amyloid β-peptide (Aβ).[1] Aβ is derived from the membrane-spanning βAPP (Kang *et al.*, 1987). Four major isoforms of βAPP have been described which are all derived by alternative splicing. In addition to the 695-amino acid form (Kang *et al.*, 1987), three other major forms have been reported which contain an additional exon encoding a protease inhibitory domain (βAPP 563, 751, and 770) (Kitaguchi *et al.*, 1988; Ponte *et al.*, 1988; Tanzi *et al.*, 1988; DeSauvage and Octave, 1989). Upon maturation of βAPP within the endoplasmic reticulum (ER) and Golgi, the precursor is cleaved by an as yet unidentified protease designated βAPP secretase to create the secreted form of βAPP (APP_s) and a 10-kDa C-terminal fragment that remains membrane-bound (Weidemann *et al.*, 1989; Oltersdorf *et al.*, 1990; Esch *et al.*, 1990; Wang *et al.*, 1991). Because this cleavage occurs within the Aβ domain, this processing pathway inhibits the formation of Aβ. In contrast, some βAPP molecules are reinternalized from the cell surface and targeted to late endosomes/lysosomes (Haass *et al.*, 1992a), where Aβ-containing C-terminal fragments of βAPP accumulate (Golde *et al.*, 1992; Estus *et al.*, 1992; Haass *et al.*, 1992a). These fragments could potentially give rise to the formation of Aβ. Recently, we and others found that Aβ is normally present in the media of cultured cells (Haass *et al.*, 1992b; Shoji *et al.*, 1992) and cerebrospinal fluid (Seubert *et al.*, 1992; Shoji *et al.*, 1992), indicating that the production and release of Aβ is a normal physiological event. In addition to the 4-kDa Aβ, we detected a 3-kDa peptide (p3) corresponding to a truncated fragment of Aβ as well as a number of minor Aβ-related peptides (Haass *et al.* 1992b). To characterize the cellular pathways that produce the two peptides, we analyzed the formation of the peptides in pulse-chase experiments and after treatment of cultured cells with a variety of agents that interfere with cellular processing pathways. In addition, the effect of a C-terminal deletion of βAPP on the formation of Aβ and p3 was studied.

EXPERIMENTAL PROCEDURES

Drug Treatments—Colchicine was made as a 1 mM stock solution in media. Monensin was made as a 10 mM stock solution in ethanol. Leupeptin was used as described previously (Haass *et al.*, 1992a). NH_4Cl was added from a 5 M stock solution. Brefeldin A (BFA) was added from a 5 mg/ml stock solution in ethanol. For control experiments in the absence of drugs, the appropriate carrier was added. All drugs and carriers were diluted into the media before the mixture was applied to the cells. Human embryonic kidney 293 cells stably transfected with βAPP 695 (Selkoe *et al.*, 1988) were incubated during a 16-h labeling period in methionine-free media containing 10% fetal calf serum with the corresponding drugs (colchicine, leupeptin, monensin, NH_4Cl). Identical results were obtained during a 3-h pulse label in the presence of the corresponding drug. Experiments using BFA were carried out only in a 3-h pulse-labeling experiment. All experiments were repeated three to nine times. Metabolic labeling and immunoprecipitations from cell extracts and media were performed as described (Haass *et al.*, 1991, 1992b). Immunoprecipitated APP_s was separated on a 10% SDS-polyacrylamide gel, whereas Aβ and p3 were separated on a 10–20% Tris-Tricine gel (Haass *et al.*, 1992b). Autofluorography was carried out as described (Haass *et al.*, 1991). The inhibitory effect of drugs on the formation of Aβ and p3 was quantified by densitometry.

Antibodies Used for Immunoprecipitation—The polyclonal antibody C7 (Podlisny *et al.*, 1991) is directed against the last 20 amino acids of the cytoplasmic tail of βAPP. This antibody immunoprecipitates N'- and N' plus O'-glycosylated full-length βAPP, the 10-kDa and a variety of potentially amyloidogenic C-terminal fragments (Haass *et al.*, 1992a). The affinity-purified polyclonal antibody B5 (Oltersdorf *et al.*, 1990) was raised to a recombinantly expressed protein of $βAPP^{444-592}$ (numbering of βAPP 695; Kang *et al.* (1987))

* This work was supported by National Institutes of Health Grants AG 06173 (LEAD Award) and AG 07911 (to D. J. S.), a grant from the Deutsche Forschungsgemeinschaft (to C. H.), and a grant from Merck Sharp and Dohme Research Laboratories (to A. Y. H.). The costs of publication of this article were defrayed in part by the payment of page charges. This article must therefore be hereby marked "*advertisement*" in accordance with 18 U.S.C. Section 1734 solely to indicate this fact.

‡ Present address: Research Unit of Experimental Neuropathology, Austrian Academy of Science, Institute of Neurology, Vienna A1090, Austria.

[1] The abbreviations used are: Aβ, amyloid β-peptide; βAPP, β-amyloid precursor protein; APP_s, soluble βAPP; BFA, brefeldin A; PCR, polymerase chain reaction; Tricine, *N*-tris(hydroxymethyl)methylglycine; ER, endoplasmic reticulum.

and immunoprecipitates APP_s and N'- and N' plus O'-glycosylated full-length βAPP. The polyclonal antibody R1280 (Tamaoka *et al.*, 1992) was raised to synthetic $Aβ^{1-40}$. This antibody immunoprecipitates Aβ, p3, and small amounts of APP_s from media of tissue-culture cells (Haass *et al.*, 1992b).

Construction of a βAPP C-terminal Deletion Construct and Transfection—A cDNA construct was designed to encode a truncated species of βAPP by introducing a stop codon after amino acid 653 of βAPP 695. The stop codon was introduced by using the oligonucleotide CCTCTAGACTAGTACTGTTTCTTCTT (underlined sequence = *Xba*I site; bold letters = STOP codon) as a 3′ primer and the 5′ oligonucleotide GATGCAGAATTCCGACAT (underlined sequence = *Eco*RI site) as a primer for a polymerase chain reaction (PCR). The PCR products were digested with *Eco*RI and *Xba*I and subcloned into the *Eco*RI/*Spe*I-linearized CMV695 plasmid (Selkoe *et al.*, 1988) creating CMV695ΔC. The sequence was confirmed by sequencing both strands of the PCR product. Transient transfections into 293 cells were performed using Lipofectin (GIBCO/BRL) as described by the manufacturer.

RESULTS AND DISCUSSION

As a model system to analyze the cellular pathways which result in the production of Aβ and p3, we used human kidney 293 cells stably transfected with a βAPP 695 cDNA. These cells are known to process βAPP in a manner similar to primary human endothelial cells (Haass *et al.*, 1992a). It should be noted that Aβ and p3 are normally produced by a variety of primary cells and untransfected cell lines, including kidney 293 cells (Seubert *et al.*, 1992; Haass *et al.*, 1992b), thus excluding the possibility that these peptides are produced by aberrant processing due to βAPP overexpression in transfected cells.

To examine the release of Aβ and p3, 293 cells stably transfected with a βAPP 695 cDNA (Selkoe *et al.*, 1988) were pulse-labeled with [^{35}S]methionine and chased in the presence of excess unlabeled methionine for various times. Aβ and p3 were immunoprecipitated from the conditioned media using R1280, a high titer antibody against synthetic $Aβ^{1-40}$ (Tamaoka *et al.*, 1992). As a control, APP_s was immunoprecipitated from equal aliquots of the same samples using antibody B5 to recombinant $βAPP^{444-592}$ (Oltersdorf *et al.*, 1990). Aβ and p3 were generated at rates similar to that of APP_s (Fig. 1). The concomitant appearance of Aβ and p3 suggests that no precursor-product relationship exists between the two peptides. This conclusion is supported by the observation that even after a 2-h label-free chase no decrease of Aβ or increase of p3 was observed, indicating that Aβ was not converted to p3 (Fig. 1). The results suggest that the two peptides are formed via parallel mechanisms from different βAPP molecules or degradative intermediates. Furthermore, the data suggest that p3 could be derived from the 10-kDa C-terminal fragment following secretory cleavage of APP_s, and not from Aβ. This possibility is supported by our previous radiosequencing of p3, which showed that its N terminus is either at the secretase cleavage site or 1 amino acid C-terminal to this site (Haass *et al.*, 1992b). Nevertheless, our experiments do not rule out the possibility that Aβ and p3 are both derived from one common precursor, *e.g.* a ~100-amino acid-long C-terminal fragment that can be differentially cleaved.

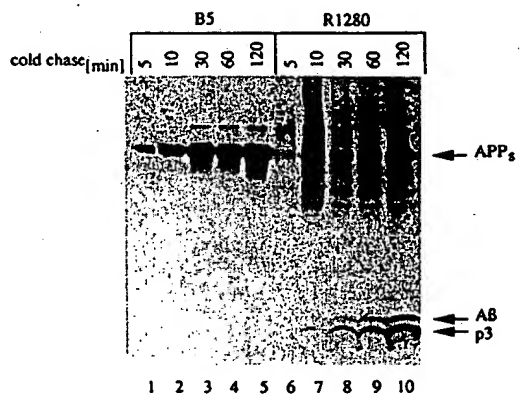

FIG. 1. **Aβ and p3 are released in parallel in a pulse-chase experiment.** Kidney 293 cells were pulse-labeled for 20 min with 100 μCi/ml [^{35}S]L-methionine and chased for 5, 10, 30, 60, and 120 min in the presence of excess amounts of unlabeled methionine. An aliquot of each sample was immunoprecipitated with antibody B5 (*lanes 1–5*), and the remaining supernatants were immunoprecipitated with antibody R1280 (*lanes 6–10*).

To analyze the cellular mechanisms involved in the formation of the two peptides in greater detail, we studied the effect of a variety of drugs on the production of Aβ and p3 by 293 cells stably transfected with βAPP 695. Since microtubule depolymerizing agents are known to inhibit transport vesicles from fusing with prelysosomal compartments (Kelly, 1990), we analyzed the formation of Aβ and p3 upon treatment of cells with colchicine and nocodazole. Colchicine (Fig. 2*A*) and nocodazole (data not shown) had no significant effect on the production of Aβ and p3, despite the fact that immunocytochemical experiments using anti-tubulin antibodies revealed a complete depolymerization of the microtubular cytoskeleton (data not shown).

To determine whether lysosomal proteases may be involved in the generation of Aβ and p3, 293 cells were treated with leupeptin. Increasing amounts of leupeptin had no influence on the generation of both peptides (Fig. 2*B*), despite the fact that this drug causes a substantial accumulation of Aβ-containing C-terminal fragments of βAPP in the lysosomes of these cells (Haass *et al.*, 1992a). In contrast, increasing amounts of NH_4Cl clearly inhibited the formation of Aβ (~78% at the maximum concentration) with less inhibition of p3 formation (~49% at the maximum concentration; Fig. 2*C*), indicating that an acidic cellular compartment is involved in the generation of Aβ. The monovalent ionophore monensin, which is known to abolish H^+, Na^+, and K^+ gradients and thus inhibit late Golgi and lysosomal functions (Tartakoff, 1983), had a strong dose-dependent inhibitory effect on the formation of Aβ (~96% at the maximum concentration), with less effect on p3 formation (~67% at the maximum concentration; Fig. 2*D*). In parallel, monensin also down-regulated APP_s secretion (Fig. 2*D*) and inhibited the maturation of intracellular βAPP, resulting in a marked accumulation of an incompletely mature form of βAPP within the cell (Fig. 2*E*) and low level secretion of incompletely mature APP_s (see down-shift in apparent molecular mass of APP_s upon monensin treatment in Fig. 2*D*). The small amount of C-terminal 10-kDa fragment seemed to be stabilized by monensin (Fig. 2*E*), suggesting an inhibition of the lysosomal degradation of this fragment. The effect of monensin on the maturation of intracellular βAPP is similar to that reported by Caporaso *et al.* (1992). The drug experiments described above were carried out by incubating the cells with drugs during a 16-h period of metabolic labeling. Repetition using a 3-h pulse-labeling experiment gave essentially the same results (data not shown). The latter experiments rule against the possibility that a 16-h treatment with these drugs leads to reduced viability of the tissue culture cells.

The possibility of Aβ formation within the ER or early Golgi was excluded by the use of brefeldin A (BFA), which causes a redistribution of Golgi into ER (Pelham, 1991). Under these conditions, Aβ and p3 could not be detected either in the media (Fig. 2*F*) or inside the cell. As expected, maturation of full-length βAPP was inhibited, resulting in an

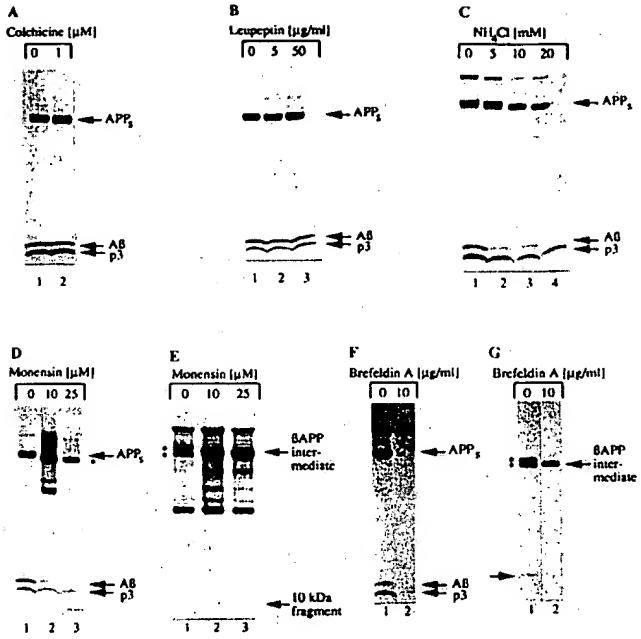

FIG. 2. **The effect of colchicine, leupeptin, NH_4Cl, monensin, and brefeldin A on the production of Aβ and p3.** *A*, colchicine does not inhibit the formation of Aβ and p3. Kidney 293 cells were treated with no colchicine (*lane 1*) or 1 μM colchicine (*lane 2*). *B*, increasing amounts of leupeptin had no influence on the formation of Aβ and p3. *Lane 1*, control; *lane 2*, 5 μg/ml; *lane 3*, 50 μg/ml. *C*, increasing amounts of NH_4Cl inhibit the formation of Aβ, with less effect on p3. *Lane 1*, control; *lane 2*, 5 mM; *lane 3*, 10 mM; *lane 4*, 20 mM. *D*, increasing amounts of monensin inhibit the formation of Aβ, with less effect on p3. *Lane 1*, control; *lane 2*, 10 μM; *lane 3*, 25 μM. *Asterisk* indicates immature form of APP_s. *E*, monensin inhibits the normal maturation of βAPP. Cell extracts from the experiment shown in *panel D* were immunoprecipitated with an antibody (C7) raised against the C terminus of βAPP (Podlisny *et al.*, 1991). *Asterisks* indicate *N'*- and *N'* plus *O'*-glycosylated βAPP in untreated control cells. *Lane 1*, control; *lane 2*, 10 μM; *lane 3*, 25 μM. *F*, BFA completely inhibits the production of p3 and Aβ. *Lane 1*, control; *lane 2*, 10 μg/ml BFA. *G*, BFA inhibits the maturation of cellular βAPP. Cell extracts from the experiment shown in *panel F* were immunoprecipitated with antibody C7. *Lane 1*, control; *lane 2*, 10 μg/ml BFA. *Asterisks* indicate *N'*- and *N'* plus *O'*-glycosylated βAPP in untreated control cells. *Lower arrow*, 10-kDa C-terminal fragment. The 200-kDa proteins detected in all immunoprecipitations and the 45-kDa protein in *E* are nonspecific proteins, which are unrelated to βAPP and are also precipitated with irrelevant antibodies (Haass *et al.*, 1992b).

incompletely glycosylated βAPP molecule (Fig. 2*G*). These experiments also exclude the possibility that Aβ might be formed within the cytoplasm after incomplete translocation of βAPP into the ER, since such a process would be unaffected by BFA.

Interestingly, we could not detect any intracellular Aβ in the extracts of the cells treated with each of the different drugs described above (data not shown), a finding consistent with previous data (Shoji *et al.*, 1992; Haass *et al.*, 1992b).

To determine the influence of the cytoplasmic domain of βAPP, which contains a potential consensus sequence for coated pit-mediated reinternalization of cell surface proteins (NPXY; Chen *et al.* (1990)), on the formation of Aβ and p3, a stop codon was inserted after position 653 (numbering according to βAPP 695; Kang *et al.* (1987)), giving rise to C-terminal truncated βAPP. This construct (named CMV695ΔC) and the wild type cDNA (CMV695) were transfected into 293 cells, followed by metabolic labeling and immunoprecipitation by R1280 and B5 (Fig. 3). Immunoprecipitation of APP_s by antibody B5 revealed that deletion of the cytoplasmic tail resulted in increased secretion of APP_s (Fig. 3*A*). This observation may be explained by the fact that the truncated protein has been shown to undergo a reduced rate of reinternalization from the cell surface,[2] thus providing more substrate to βAPP secretase, which has been reported to cleave βAPP at least in part on the cell surface (Sisodia, 1992; Haass *et al.*, 1992a). Such an increase of APP_s secretion following the deletion of the C terminus has also been mentioned by Sisodia (1992). This increase in APPs is paralleled by increased release of p3 (Fig. 3*B*). This is consistent with the hypothesis that p3 is derived from the C-terminal fragment of βAPP created by secretase, because enhanced cleavage of full-length βAPP should create more of the 10-kDa C-terminal fragment. Furthermore, in the absence of the C terminus, Aβ is still produced, although in smaller amounts. Interestingly, radiosequencing of this 4-kDa band demonstrated that, in addition to Aβ, significantly increased amounts of 4-kDa Aβ-related peptides were observed. These peptides began at Val (−3) and Arg (5), relative to the Aβ sequence (data not shown). These data show that an intact cytoplasmic domain of βAPP is not absolutely necessary for the formation and release of either p3 or Aβ or Aβ-related peptides. In addition, these experiments strongly suggest that p3 and Aβ are derived from different precursor molecules, and that p3 does not derive simply by proteolytic cleavage of Aβ at the secretase site, since the amounts of p3 and Aβ do not change in parallel.

Our data indicate that an acidic compartment is involved at some point in the formation of Aβ and also in part in the formation of p3. This is supported by the fact that NH_4Cl and monensin reduce the amounts of both peptides. Furthermore, the pulse-chase experiment together with the results of monensin treatment suggest that only completely mature βAPP can give rise to the formation of Aβ. The production of Aβ and p3 in the ER or early Golgi is excluded by the use of BFA. Shoji *et al.* (1992) have postulated that lysosomes may

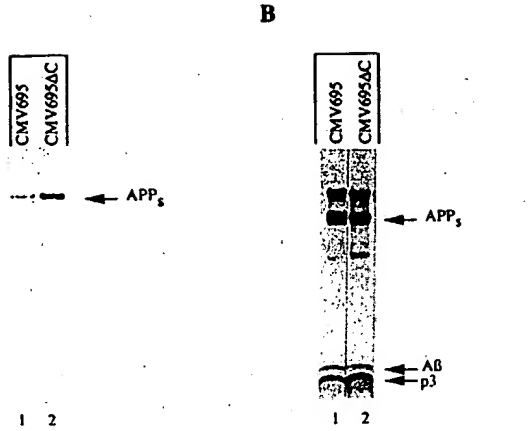

FIG. 3. **Deletion of the cytoplasmic domain of βAPP causes an increase in APP_s secretion and production of p3.** *A*, deletion of the C terminus of βAPP causes an increased secretion of APP_s. Kidney 293 cells were transfected with CMV695 (*lane 1*) or CMV695ΔC (*lane 2*), and the media from the metabolically labeled cells were immunoprecipitated with B5. *B*, p3 and Aβ are detected in the medium of cells transfected with CMV695ΔC. Kidney 293 cells were transfected with CMV695 (*lane 1*) or CMV695ΔC (*lane 2*), and the media from the metabolically labeled cells were immunoprecipitated with R1280. Cotransfection with a plasmid encoding the human growth hormone (Nichols Institute) confirmed similar transfection efficiencies with CMV695 and CMV695ΔC.

[2] E. Koo, personal communication.

be involved in the generation of Aβ. This is based on the observation that NH_4Cl decreases the amounts of Aβ. However, leupeptin did not have any effect on the formation of Aβ (Shoji *et al.*, 1992). The fact that leupeptin and colchicine/nocodazole do not inhibit the formation of both peptides in the present experiments indicates that lysosomes may not be directly involved in the proteolytic processing that results in the formation of either p3 or Aβ. This conclusion is further supported by the fact that we were unable to detect the two peptides within isolated lysosomes purified from metabolically labeled 293 cells (data not shown). Furthermore, leupeptin strongly increases the amounts of the 10-kDa C-terminal fragment and larger potentially amyloidogenic fragments within the lysosome (Caporaso *et al.*, 1992; Golde *et al.*, 1992; Haass *et al.*, 1992a). Despite this accumulation of very high amounts of the 10-kDa C-terminal fragment and slightly larger Aβ-containing fragments in the lysosome, we do not observe higher amounts of p3 or Aβ in the media. We hypothesize that only prelysosomal 10-kDa fragments (most likely on or near the cell surface) and larger Aβ-containing precursor fragments can give rise to p3 and Aβ, respectively. One could argue that leupeptin treatment could inhibit the formation of both peptides within the lysosome, but this should result in reduced amounts of the two peptides upon leupeptin treatment, a finding which is clearly not the case (see Fig. 2*B*).

The hypothesis that lysosomal degradation of βAPP is not an absolute prerequisite for Aβ production is further supported by the finding that cultured fibroblasts from patients with I-cell disease, which are unable to target proteases directly to lysosomes, still produce Aβ.[3] Our data do not exclude the possibility that full-length βAPP or Aβ-bearing fragments thereof might be reinternalized from the cell surface, giving rise to Aβ and p3 within an early endocytic vesicle that subsequently recycles to the cell surface and releases the peptides into the medium.

As a working model, we propose the possibility that the cleavage producing the N terminus of Aβ may be mediated by alternative cleavage of mature βAPP by the secretase or a closely related enzyme within late Golgi and/or cell surface. This event could take place either on the cell surface or within the acidic compartments of late Golgi or transport vesicles derived from a reinternalization pathway carrying βAPP or fragments thereof. Indeed, evidence has recently been presented that alternative secretory cleavage of βAPP may potentially create the N terminus of Aβ (Seubert *et al.*, 1993).

[3] C. Haass, T. Oltersdorf, I. Lieberburg, and D. Selkoe, unpublished data.

Acknowledgment—We thank Dr. E. Koo for helpful suggestions.

REFERENCES

Caporaso, G. L., Gandy, S. E., Buxbaum, J. D., and Greengard, P. (1992) *Proc. Natl. Acad. Sci. U. S. A.* **89**, 2252–2256
Chen, W. J., Goldstein, J. L., and Brown, M. S. (1990) *J. Biol. Chem.* **265**, 3116–3123
DeSauvage, F., and Octave, J.-N. (1988) *Science* **245**, 651–653
Esch, F. S., Keim, P. S., Beattie, E. C., Blacher, R. W., Culwell, A. R., Oltersdorf, T., McClure, D., and Ward, P. J. (1990) *Science* **248**, 1122–1124
Estus, S., Golde, T. E., Kunishita, T., Blades, D., Lowery, D., Eisen, M., Usiak, M., Qu, X., Tabira, T., Greenberg, B. D., and Younkin, S. G. (1992) *Science* **255**, 726–728
Golde, T. E., Estus, S., Younkin, L. H., Selkoe, D. J., and Younkin, S. G. (1992) *Science* **255**, 728–730
Haass, C., Hung, A. Y., and Selkoe, D. J. (1991) *J. Neurosci.* **11**, 3783–3793
Haass, C., Koo, E. H., Mellon, A., Hung, A. Y., and Selkoe, D. J. (1992a) *Nature* **357**, 500–503
Haass, C., Schlossmacher, M. G., Hung, A. Y., Vigo-Pelfrey, C., Mellon, A., Ostaszewski, B. L., Lieberburg, I., Koo, E. H., Schenk, D., Teplow, D. B., and Selkoe, D. J. (1992b) *Nature* **359**, 322–325
Kang, J., Lemaire, H. G., Unterbeck, A., Salbaum, J. M., Masters, C. L., Grzeschik, K. H., Multhaup, G., Beyreuther, K., and Müller-Hill, B. (1987) *Nature* **325**, 73 3–736
Kelly, R. B. (1990) *Cell* **61**, 5–7
Kitaguchi, N., Takahashi, Y., Tokushima, Y., Shiojiri, S., and Ito, H. (1988) *Nature* **331**, 530–532
Oltersdorf, T., Ward, P. J., Henriksson, T., Beattie, E. C., Neve, R., Lieberburg, I., and Fritz, L. C. (1990) *J. Biol. Chem.* **265**, 4492–4497
Pelham, H. R. B. (1991) *Cell* **67**, 449–451
Podlisny, M. B., Tolan, D. R., and Selkoe, D. J. (1991) *Am. J. Pathol.* **138**, 1423–1435
Ponte, P., Gonzales-DeWhitt, P., Schilling, J., Miller, J., Hsu, D., Greenberg, B., Davis, K., Wallace, W., Lieberburg, I., Fuller, F., and Cordell., B. (1988) *Nature* **331**, 525–527
Selkoe, D. J., Podlisny, M. B., Joachim, C. L., Vickers, E. A., Lee, G., Fritz, L., and Oltersdorf, T. (1988) *Proc. Natl. Acad. Sci. U. S. A.* **85**, 7341–7345
Seubert, P., Vigo-Pelfrey, C., Esch, F., Lee, M., Dovey, H., Davis, D., Sinha, S., Schlossmacher, M., Whaley, J., Swindlehurst, C., McCormack, R., Wolfert, R., Selkoe, D., Lieberburg, I., and Schenk, D. (1992) *Nature* **359**, 325–327
Seubert, P., Oltersdorf, T., Lee, M. G., Barbour, R., Blomquist, C., Davis, D. L., Bryant, K., Fritz, L. C., Galasko, D., Thal, L. J., Lieberburg, I., and Schenk, D. (1993) *Nature*, in press
Shoji, M., Golde, T. E., Cheung, T. T., Ghiso, J., Estus, S., Shaffer, L. M., Cai, X. D., McKay, D. M., Tintner, R., Frangione, B., and Younkin, S. G. (1992) *Science* **258**, 126–129
Sisodia, S. S. (1992) *Proc. Natl. Acad. Sci. U. S. A.* **89**, 6075–6079
Tamaoka, A., Kalaria, R. N., Lieberburg, I., and Selkoe, D. J. (1992) *Proc. Natl. Acad. Sci. U. S. A.* **89**, 1345–1349
Tanzi, R. E., McClatchey, A. I., Lamperti, E. D., Villa-Kamaroff, L. L., Gusella, J. F., and Neve, R. L. (1988) *Nature* **331**, 528–530
Tartakoff, A. M. (1983) *Cell* **32**, 1026–1028
Wang, R., Meschia, J. F., Cotter, R. J., and Sisodia, S. S. (1991) *J. Biol. Chem.* **266**, 16960–16964
Weidemann, A., König, G., Bunke D., Fischer, P., Salbaum, J. M., Masters, C. L., and Beyreuther, K. (1989) *Cell* **57**, 115–126